Ultra-marginal Feature Importance: Learning from Data with Causal Guarantees

Joseph Janssen
University of British Columbia

Vincent Guan
University of British Columbia

Elina Robeva
University of British Columbia

Abstract

Scientists frequently prioritize learning from data rather than training the best possible model; however, research in machine learning often prioritizes the latter. Marginal contribution feature importance (MCI) was developed to break this trend by providing a useful framework for quantifying the relationships in data. In this work, we aim to improve upon the theoretical properties, performance, and runtime of MCI by introducing ultra-marginal feature importance (UMFI), which uses dependence removal techniques from the AI fairness literature as its foundation. We first propose axioms for feature importance methods that seek to explain the causal and associative relationships in data, and we prove that UMFI satisfies these axioms under basic assumptions. We then show on real and simulated data that UMFI performs better than MCI, especially in the presence of correlated interactions and unrelated features, while partially learning the structure of the causal graph and reducing the exponential runtime of MCI to super-linear.

1 INTRODUCTION

Scientists often seek to understand the relationships between a set of characteristics and some outcome of interest (Kruskal, 1984). These relationships are ideally determined by performing carefully controlled experiments so that causality can be established. However, experiments can be difficult and costly to pursue, unethical to perform, or impossible to control (Wright, 1921; Vowels et al., 2021), leaving only observational data available. The relationships that are hidden within vast quantities of observational data are often difficult to determine, so statistical tools, such as feature importance, have been explored.

Proceedings of the 26[th] International Conference on Artificial Intelligence and Statistics (AISTATS) 2023, Valencia, Spain. PMLR: Volume 206. Copyright 2023 by the author(s).

Recently, feature importance methods such as Shapley values (Shapley, 1953; Cohen et al., 2007; Lundberg and Lee, 2017), Shapley additive global importance (SAGE) (Covert et al., 2020), accumulated local effects (ALE) (Apley and Zhu, 2020), permutation importance (PI) (Breiman, 2001), and conditional permutation importance (CPI) (Debeer and Strobl, 2020), have been used in high-impact journal papers by scientists who want to explain the mechanisms behind observational data (Addor et al., 2018; Bazaga et al., 2020; Stein et al., 2021; Johnsen et al., 2021; Schmidt et al., 2020; Gill et al., 2017; Janssen et al., 2022). However, these methods are predominantly for model explanation or feature selection, so they have many shortcomings when used for other purposes such as scientific inference (Freiesleben et al., 2022; Catav et al., 2021). ALE can nicely display how changes in inputs lead to altered model predictions but important higher order effects are omitted (Molnar, 2020), and although CPI improves upon some limitations of PI, CPI gives zero importance to perfectly correlated features even if they offer significant explanatory power towards the response (Covert et al., 2020). Similarly, Shapley values diminish the importance of duplicated or highly correlated features (Catav et al., 2021). Further, only one model is trained in ALE, CPI, and PI. Thus, correlated features, which can alter the model assembly process, could be given artificially low importance if the goal is to explain the data (Hooker et al., 2021). Due to the multiplicity of near optimal models with vastly different functioning, one cannot use a single model to explain the data generating processes (Marx et al., 2022; Molnar et al., 2021). Instead of exploring a single model, the developers of SAGE, SPVIM, and marginal contribution feature importance (MCI) evaluate the difference in accuracy between a model trained with the feature of interest and a model trained without it, across all feature subsets (Catav et al., 2021; Covert et al., 2020; Williamson and Feng, 2020). However, these methods have not been accepted by a wider scientific audience because of their high computational cost. In particular, we note that MCI is a recently developed method for explaining data, and it was shown in extensive experiments to have better quality and robustness when compared to Shapley values, SAGE, ablation, and bivariate methods (Catav et al., 2021).

Although MCI is a powerful and innovative method for ex-

plaining data, it has three key shortcomings. First, MCI demands an exponential number of model trainings, making it unsuitable even for small-to-medium-sized datasets. Second, although it can handle complex feature interactions and data with correlated features, MCI underestimates the importance of correlated features that form interaction effects because MCI usually ignores features that share information with the feature of interest, as explained further in Section 4.1.2. Third, MCI can give non-zero importance to features that are completely unrelated to the response variable, as experimentally shown in Catav et al. (2021, Figure S3) and theoretically shown in Harel et al. (2022). We hypothesize that constructing information-preserving representations of the data that are independent of the feature of interest could resolve these three issues. With this in mind, we introduce ultra-marginal feature importance (UMFI), a new variable importance method that can better describe data while drastically reducing runtime.

The rest of this paper is organized as follows. Axioms for explaining data are proposed in Section 2. The framework for UMFI is then formally presented in Section 3 along with its theoretical properties and its simple algorithm. In Section 4, we conduct experiments on simulated and real data to assess the quality, robustness, and time complexity of UMFI compared to MCI. Finally, an overview of the work, its limitations, and ideas for future work are discussed in Section 5.

Related Work

This paper is greatly inspired by the development of marginal contribution feature importance (MCI) by Catav et al. (2021). Let $F = \{x_1, ..., x_p\}$ be the set of features used to predict the response variable, y. The universal predictive power of a set of features $S \subseteq F$ is given by

$$\nu(S) = \min_{f \in G(\emptyset)} \mathbb{E}[l(f(\emptyset), y)] - \min_{f \in G(S)} \mathbb{E}[l(f(S), y)], \quad (1)$$

where l is a specified loss function and $G(S)$ is the set of all predictive models restricted to using features in $S \subseteq F$. ν is closely related to mutual information, with equality under ideal conditions (Covert et al., 2020), but in practice, ν is often approximated by machine learning evaluation functions (Covert et al., 2020; Catav et al., 2021). Using this, Catav et al. (2021) defined the marginal contribution feature importance (MCI) of a feature $x_i \in F$ as

$$I_\nu(x_i) = \max_{S \subseteq F} \quad \nu(S \cup \{x_i\}) - \nu(S). \quad (2)$$

To achieve our goal of improving upon the shortcomings of MCI, we evaluate the importance of a feature of interest x_i after preprocessing the data to remove dependencies on x_i. Finding independent representations of predictors for creating improved feature importance methods is a novel objective, though similar ideas have been alluded to as future work in König et al. (2021), Chen et al. (2020), and Fan and Lv (2008). The weaker concept of finding orthogonal representations of data has been discussed previously (Gibson, 1962), though the discussion has been limited to relative importance measures for multiple linear regression (Bi, 2012; Wurm and Fisicaro, 2014). Methods which can not only orthogonalize features, but also remove more general dependencies, have seen great progress within the domains of AI fairness and privacy. Some examples of these *preprocessing* techniques include regression (Bird et al., 2020), optimal transport (Johndrow and Lum, 2019), neural networks (Song et al., 2019; Moyer et al., 2018; Gitiaux and Rangwala, 2021b,a), convex optimization (Calmon et al., 2017), kernels (Tan et al., 2020), and principal inertial components (Wang and Calmon, 2017). Linear regression and optimal transport are used in this paper. Gurushankar et al. (2022) studies the problem of using fairness techniques to perform partial information decomposition, which leads to interesting connections with our work.

2 AXIOMS FOR EXPLAINING DATA

2.1 Background and Notation

We use x_i to denote an observed feature from the feature set F, and X_i to denote the random variable that x_i is sampled from. Suppose that $(F, y) = (x_1, ..., x_p, y)$ is sampled jointly from the joint distribution (X_{obs}, Y), where $X_{obs} \subseteq X_{full} = \{X_1, X_2, ...X_r\}$, and $p \leq r$. To accommodate dependency removal, we will require that the universal predictive power ν, defined in Equation (1), is also defined for transformations of the feature set. We therefore define the space of *information subsets* of a feature set F as

$$\mathcal{I}(F) = \{g(F) : g \text{ is a deterministic function of } F\}. \quad (3)$$

We call these information subsets of F because $I(Y; g(F)) \leq I(Y; F)$ holds for any deterministic function g by Theorem A.5.

Given the data (F, y) and an evaluation function ν, the feature importance of $x_i \in F$ is denoted by

$$Imp_\nu^{F,y}(x_i) \in \mathbb{R}_{\geq 0}. \quad (4)$$

In contrast to X_{obs}, we assume that X_{full} is causally sufficient, meaning that there are no latent confounders in the underlying data generating process (Yu et al., 2018). Hence, we may consider the full causal graphical model with graph $G = (V, E)$, such that each vertex from $V = \{1, ..., r+1\}$ is associated to a random variable from $X_{full} \cup Y := \{V_1, ..., V_r, V_{r+1}\}$, and the directed edge set E enables the graphical model to obey the global Markov property (Kang and Tian, 2009). The graphical model can

often be given by a structural causal model $C = (G, U, \mathcal{E})$, where G is as defined above, $\mathcal{E}$ is a set of mutually independent noise variables $\epsilon_1, ..., \epsilon_{r+1}$, and $U = \{u_1, ..., u_{r+1}\}$ is the set of functions relating the variables $V_1, ..., V_{r+1}$ to their parents in G via the relation $V_i = u_i(V_{pa(i)}, \epsilon_i)$.

2.2 Axioms

Any attempt to build a method that explains the data should begin by rigorously defining what explaining the data truly means. Different, but closely related definitions and goals have been formulated by Chen et al. (2020), Catav et al. (2021), Grömping (2009), Bénard et al. (2022), and Tološi and Lengauer (2011). Inspired by the above works, we provide three intuitive axioms for feature importance methods intended for explaining data and scientific inference.

1. **Elimination axiom:** Eliminating a feature x_j from F can only decrease the importance of other features:

$$\forall x_i \in F \setminus \{x_j\}, Imp_\nu^{F\setminus\{x_j\},y}(x_i) \leq Imp_\nu^{F,y}(x_i).$$

2. **Invariance under Redundant Information and Symmetry under Duplication (IRI & SD) axiom:** Let $\hat{x}$ be a redundant feature, i.e. $\hat{x} \in \mathcal{I}(F)$. Then adding $\hat{x}$ to the feature set F to create $F' = F \cup \hat{x}$ will not change the importance given to any preexisting feature in F. Also, in the case where the added feature $\hat{x}$ is a duplicate of a preexisting feature $x_j \in F$ (i.e., $\hat{x} = h(x_j)$ and h is bijective) both $\hat{x}$ and x_j will be given equal importance:

$$\hat{x} \in \mathcal{I}(F) \implies Imp_\nu^{F,y}(x_i) = Imp_\nu^{F',y}(x_i)\ \forall x_i \in F$$

$$\hat{x} = h(x_j) \implies Imp_\nu^{F',y}(\hat{x}) = Imp_\nu^{F',y}(x_j).$$

3. **Blood relation axiom:** A feature x_i will be given non-zero and positive importance if and only if it is blood related to the response Y in the full causal graphical model $G = (V, E)$. Two vertices are said to be blood related if there is a directed path between them or if there is a backdoor path between them via a common ancestor. Figure 2 illustrates an example.

$$Imp_\nu^{F,y}(x_i) > 0 \iff X_i \in BR_G(Y).$$

The *elimination axiom* comes directly from Catav et al. (2021). Once a feature is observed to be related to the response, the relationship strength between the feature and response should not drop, regardless of the additional features added. In fact, the importance should often increase, since adding features could reveal further synergistic information about the response (Griffith and Koch, 2014; Williams and Beer, 2010). Hence, the elimination axiom suggests that a feature importance method intended for scientific inference should be expressive enough to capture complex feature interactions.

The *invariance under redundant information (IRI)* portion of our second axiom is a generalization of the duplication invariance property introduced in Catav et al. (2021) and the group size invariance property introduced in Tološi and Lengauer (2011). If a dataset contains two duplicate features, a model may use them equally often and therefore divide the importance equally between them (random forests), or only one of the features may be given importance (lasso) (Chen et al., 2020). However, from the data's perspective, the original importance found before duplication should be maintained (Tološi and Lengauer, 2011; Catav et al., 2021). Further, after adding duplicate features, no additional interaction capability is available (Griffith and Koch, 2014), so the importance of all other features should remain the same. The same arguments can be made for features offering only redundant information, which arise much more frequently than exact duplicates, thus motivating IRI. The *symmetry under duplication (SD)* aspect of our second axiom is functionally equivalent to the symmetry property presented in Catav et al. (2021) and is similar to the correlated group property in Tološi and Lengauer (2011). The purpose of this part of the axiom, as pointed out by Tološi and Lengauer (2011), is to prevent the feature importance method from dismissing features that are not needed for better predictions, but which may be part of the true underlying causal model.

We call the final axiom the *blood relation axiom* because it asserts that a feature should have non-zero importance with respect to the response y if and only if it is connected to y in the causal graph through a directed path or via a common ancestor, much like how blood relatives are connected within a family tree. This axiom suggests that feature importance scores intended for data explanation should extract reliable knowledge about the underlying causal graph and data generating process. When two features are blood related, or equivalently, when there is an open path between them, the two features are said to be associated (see Greenland et al. (1999) and Williams et al. (2018)). Thus, a feature importance metric satisfying this axiom would give non-zero importance to a feature if and only if there is a statistical association between that feature and the response. Statistical association is not only a quality of interest for many applications (e.g., genome-wide association studies), it also forms the foundation of Pearl's causal hierarchy (Shpitser and Pearl, 2008). Some may argue that we should only assign importance to features with a directed path to the response, but as pointed out by Grömping (2009), even if this were desired, this is an impossible goal since $X \to Z \to Y$ is Markov equivalent to $X \leftarrow Z \to Y$. It is argued by Grömping (2009) that any importance measure aimed at explanatory or causal purposes must give importance to X and Z in both scenarios.

Additionally, a feature importance metric satisfying this axiom can partition the feature set into features that are

blood related to the response and features that are not blood related to the response. Although it does not enable us to immediately recover the full causal graph, this partitioning may be a helpful supplemental tool for other fast partial causal graph discovery methods (Soleymani et al., 2022). This would be an especially relevant research direction since Reisach et al. (2021) recently showed that classic causal discovery algorithms are more inaccurate than previously thought. This partitioning could also be useful for sure independence screening (Fan and Lv, 2008; Schellhas et al., 2020).

The axioms introduced in this section are only intended to define ideal properties for feature importance methods that are focused on scientific inference. We do not claim that a unique solution exists since all three axioms are invariant to scalar multiplication, nor do we claim that a method exists that satisfies all axioms in all scenarios.

3 ULTRA-MARGINAL FEATURE IMPORTANCE

Let $F = \{x_1, ..., x_p\}$ be a set of p features of arbitrary type used to predict the response Y.

Definition 1. *We denote $S^F_{x_i}$ as a preprocessed feature set after dependencies on the feature of interest x_i have been removed from F. An optimally preprocessed feature set is denoted by $\hat{S}^F_{x_i}$, and we say that a preprocessing $S^F_{x_i}$ is optimal if it obeys the following properties:*

1. $S^F_{x_i} \in \mathcal{I}(F)$
2. $S^F_{x_i} \perp\!\!\!\perp X_i$
3. $I(Y; S^F_{x_i}, X_i) = I(Y; F)$

The first property ensures that $S^F_{x_i} = g(F)$ for some deterministic function g, and hence no information from outside of F is gained during the transformation. The second property upholds that $S^F_{x_i}$ is independent of X_i. The last property affirms that there is no unnecessary information loss or distortion incurred during preprocessing (Gitiaux and Rangwala, 2022). For simplicity, we use F and $\hat{S}^F_{x_i}$ to denote both their respective data and random vector instantiations.

Provided that it exists, an optimal preprocessing $\hat{S}^F_{x_i}$ is not unique since scaling by a constant does not affect any of the optimality conditions. Therefore, given a feature of interest x_i and a feature set F, we may consider the (possibly empty) equivalence class $[\hat{S}^F_{x_i}]$ of optimal preprocessings. In practice, the last two properties of Definition 1 can be difficult to guarantee, but we later observe in Section 4 that non-optimal preprocessings can often be good enough to provide highly accurate feature importance scores for scientific inference.

Definition 2. *Given an evaluation function $\nu : \mathcal{I}(F) \to \mathbb{R}_{\geq 0}$, a feature set F, and a response y, we define the ultra-marginal feature importance (UMFI) of the feature of interest $x_i \in F$ as*

$$U^{F,y}_\nu(x_i) = \nu(S^F_{x_i} \cup \{x_i\}) - \nu(S^F_{x_i}). \tag{5}$$

We note that this definition allows for the use of any preprocessing $S^F_{x_i}$. When the utilized preprocessing $\hat{S}^F_{x_i}$ is optimal, we say that UMFI is optimally computed.

Theorem 3.1. *Suppose that the data (F, y) comes from a multivariate Gaussian distribution and that $\nu(\cdot)$ is positively linearly related to $I(Y; \cdot)$, then we can ensure that $U^{F,y}_\nu$ satisfies (i) the elimination axiom and (ii) the redundant information invariance and duplication symmetry axiom, by using linear regression to optimally compute $U^{F,y}_\nu$. If we additionally assume that the joint distribution of the variables (X_{full}, Y) is faithful to the causal graph G, then $U^{F,y}_\nu$ also satisfies (iii) the blood relation axiom.*

Proof. Since $\nu(\cdot) = aI(Y; \cdot) + b$ for some $a \geq 0$ and $b \in \mathbb{R}$, $U^{F,y}_\nu = \nu(S^F_{x_i} \cup \{x_i\}) - \nu(S^F_{x_i})$, and scaling by a constant factor does not alter any axiom, without loss of generality, it suffices to prove the axioms for the case where $\nu(\cdot) = I(Y; \cdot)$.

(i) Elimination: $U^{F\setminus\{x_j\},y}_\nu(x_i) \leq U^{F,y}_\nu(x_i)$.

Let x_j be the eliminated feature, and let $x_i \in F \setminus \{x_j\}$ be the feature of interest. Theorem C.1 in the Supplement shows that pairwise linear regression attains an optimal preprocessing $\hat{S}^F_{x_i}$ since (F, y) is multivariate Gaussian. After mean centering, pairwise linear regression transforms each feature $x_k \in F \setminus \{x_j\}$ into $\tilde{x}_k = x_k - \beta_k x_i$, where β_k is the regression coefficient of x_k on x_i. Hence, $\hat{S}^F_{x_i} = (\hat{S}^{F\setminus\{x_j\}}_{x_i}, \tilde{x}_j)$ and

$$\begin{aligned}
U^{F,y}_\nu(x_i) &= I(Y; \hat{S}^F_{x_i}, X_i) - I(Y; \hat{S}^F_{x_i}) \\
&= I(Y; \hat{S}^{F\setminus\{x_j\}}_{x_i}, \tilde{X}_j, X_i) - I(Y; \hat{S}^{F\setminus\{x_j\}}_{x_i}, \tilde{X}_j) \\
&\geq I(Y; \hat{S}^{F\setminus\{x_j\}}_{x_i}, X_i) - I(Y; \hat{S}^{F\setminus\{x_j\}}_{x_i}) \\
&= U^{F\setminus\{x_j\},y}_\nu(x_i),
\end{aligned}$$

where the inequality is given by the supermodularity of mutual information under independence (Theorem A.3), since $X_i \perp\!\!\!\perp (\hat{S}^{F\setminus\{x_j\}}_{x_i}, \tilde{X}_j)$ follows from the optimality of $\hat{S}^F_{x_i}$.

(ii) IRI: Let $\hat{x} \in \mathcal{I}(F)$, then $U^{F,y}_\nu(x_i) = U^{F\cup\{\hat{x}\},y}_\nu(x_i)$.

By the optimality of the preprocessings and the invariance of mutual information under redundant information,

$$\begin{aligned}
U^{F,y}_\nu(x_i) &= I(Y; \hat{S}^F_{x_i}, X_i) - I(Y; \hat{S}^F_{x_i}) \\
&= I(Y; F) - I(Y; \hat{S}^F_{x_i}) \\
U^{F\cup\{\hat{x}\},Y}_\nu(x_i) &= I(Y; \hat{S}^{F\cup\{\hat{x}\}}_{x_i}, X_i) - I(Y; \hat{S}^{F\cup\{\hat{x}\}}_{x_i}) \\
&= I(Y; F) - I(Y; \hat{S}^{F\cup\{\hat{x}\}}_{x_i})
\end{aligned}$$

From Lemma C.3, $[\hat{S}_{x_i}^F] \equiv [\hat{S}_{x_i}^{F\cup\{\hat{x}\}}]$. In other words, every optimal preprocessing $\hat{S}_{x_i}^F \in [\hat{S}_{x_i}^F]$ also exists in $[\hat{S}_{x_i}^{F\cup\{\hat{x}\}}]$ and vice versa. Thus, we may select the same optimal preprocessing from each equivalence class to ensure that $I(Y;\hat{S}_{x_i}^F) = I(Y;\hat{S}_{x_i}^{F\cup\{\hat{x}\}})$, which concludes the proof.

SD: Let $\hat{x} = h(x_j)$ for some bijective function h. Then, $U_\nu^{F\cup\{\hat{x}\},y}(\hat{x}) = U_\nu^{F\cup\{\hat{x}\},y}(x_j)$.

We have $U_\nu^{F\cup\{\hat{x}\},y}(\hat{x}) = I(Y;F) - I(Y;\hat{S}_{\hat{x}}^{F\cup\{\hat{x}\}})$ and $U_\nu^{F\cup\{\hat{x}\},y}(x_j) = I(Y;F) - I(Y;\hat{S}_{x_j}^{F\cup\{\hat{x}\}})$. Similarly to the proof of IRI, it suffices to show that $[\hat{S}_{x_j}^{F\cup\{\hat{x}\}}] \equiv [\hat{S}_{\hat{x}}^{F\cup\{\hat{x}\}}]$, which is proven in Lemma C.3 in the Supplement.

(iii) Blood relation: $U_\nu^{F,y}(x_i) > 0 \iff x_i \in BR_G(Y)$.

We equivalently prove $U_\nu^{F,y}(x_i) = 0 \iff X_i \notin BR_G(Y)$. First, we write $U_\nu^{F,y}(x_i) = I(Y;S_{x_i}^F, X_i) - I(Y;S_{x_i}^F) = I(Y;x_i|S_{x_i}^F)$. Also, from the definition of conditional mutual information,

$$U_\nu^{F,y}(x_i) = 0 \iff I(Y;X_i|S_{x_i}^F) = 0 \iff X_i \perp\!\!\!\perp Y|S_{x_i}^F.$$

Next, we claim that $U_\nu^{F,y}(x_i) = 0 \iff x_i \perp\!\!\!\perp Y$. A conditional independence axiom that holds for the variables in a structural causal model is the contraction axiom (Dawid, 1979): $X \perp\!\!\!\perp Y$ and $X \perp\!\!\!\perp W|Y \iff X \perp\!\!\!\perp (W,Y)$. From this, we obtain the statement

$$X_i \perp\!\!\!\perp S_{x_i}^F \text{ and } X_i \perp\!\!\!\perp Y|S_{x_i}^F \iff X_i \perp\!\!\!\perp (Y, S_{x_i}^F)$$

Since $X_i \perp\!\!\!\perp S_{x_i}^F$ is true from the optimality of the preprocessing, this property can be reduced to

$$X_i \perp\!\!\!\perp Y|S_{x_i}^F \iff X_i \perp\!\!\!\perp (Y, S_{x_i}^F) \iff X_i \perp\!\!\!\perp Y \quad (6)$$

where the last equivalence is due to $X_i \perp\!\!\!\perp S_{x_i}^F$ and the fact that $(\hat{S}_{x_i}^F, X_i, Y)$ is multivariate Gaussian (Steudel and Ay, 2015; Lauritzen and Sadeghi, 2018).

All that is left to prove is $X_i \perp\!\!\!\perp Y \iff X_i \notin BR_G(Y)$. The claim $X_i \notin BR_G(Y) \implies X_i \perp\!\!\!\perp Y$ follows from the global Markov property. Indeed, it is easy to check that X_i and Y are d-separated by the empty set in this case. The converse holds because we have assumed that the graphical model obeys faithfulness. Indeed, X_i and Y would be d-connected by the empty set if $X_i \in BR_G(Y)$. □

We note that the linear relation between $\nu(\cdot)$ and $I(Y;\cdot)$ is pivotal to the proof of Theorem 3.1. Under ideal conditions, this relationship holds (Covert et al., 2020), but in practice, the accuracy of the approximation depends on the quality of the method, the loss function, and the response variable's distribution. See Covert et al. (2021) and Supplement A.3 for a more thorough overview. Simulations have demonstrated that Gaussian graphical models with sparse graphs are generally faithful to the graph; hence, assuming faithfulness is often reasonable (Malouche and Sevestre-Ghalila, 2008).

We remark that UMFI does not require Gaussianity to satisfy all axioms. Indeed, since the last equivalence in Equation (6) can be relaxed to be an implication without Gaussianity, UMFI satisfies one direction of the blood relation axiom, $U_\nu^{F,y}(x_i) = 0 \implies x_i \notin BR_G(Y)$, for arbitrary distributions. Additionally, we show that UMFI satisfies the blood relation axiom under alternate assumptions in Supplement C. We also note that the proof of Theorem 3.1(ii) does not require the Gaussian assumption, making the IRI & SD axiom true for arbitrary distributions.

Algorithm 1: Algorithm for computing UMFI

1: Let y be the response variable of the set of predictors F. Choose a feature $x_i \in F$.
2: Obtain $S_{x_i}^F$ by using a technique that removes dependencies on x_i from F.
3: Specify a method f and a corresponding evaluation function ν_f.
4: Estimate the predictive power, $\nu_f(S_{x_i}^F)$, that $S_{x_i}^F$ has about y.
5: Estimate the predictive power, $\nu_f(S_{x_i}^F \cup \{x_i\})$, that $S_{x_i}^F \cup \{x_i\}$ has about y.
6: **return** $U_{\nu_f}^{F,y}(x_i) = \nu_f(S_{x_i}^F \cup \{x_i\}) - \nu_f(S_{x_i}^F)$

Since UMFI is model-agnostic, we provide a general algorithm, which can be applied using any pair of preprocessing functions and evaluation functions ν_f (Algorithm 1). We note that ν_f is not restricted to the domain of machine learning models or even models in general. For example, one could also implement UMFI with measures of dependence such as QMD (Griessenberger et al., 2022) or FOCI (Azadkia and Chatterjee, 2021).

4 EXPERIMENTS

We perform experiments to compare UMFI and MCI with respect to quality, robustness, and time complexity. To implement UMFI, we consider optimal transport (Johndrow and Lum, 2019) (UMFI_OT) and linear regression (Bird et al., 2020) (UMFI_LR) as methods to remove dependencies from the data. A detailed overview of these implementations is shown in Supplement E and experiments comparing their performance appear in Supplement F. For all experiments, we use random forests' out-of-bag accuracy (cross-validation R^2 for regression and cross-validation overall accuracy for classification) as the evaluation metric ν_f since it can capture nonlinearities and interaction effects (Breiman, 2001; Taufiq et al., 2023; Wright et al., 2016). We use the *ranger* package to implement random forests with 100 trees and default hyperparameters (Wright and Ziegler, 2015). All experiments were run in Microsoft R Open Version 4.0.2. Supplement G contains additional experiments comparing UMFI with other feature importance metrics including ablation, permutation importance,

and conditional permutation importance. In the same section, we rerun the experiments comparing MCI and UMFI using extremely randomized trees instead of random forests and do an additional comparison on a real dataset from hydrology (Addor et al., 2017). Code for all experiments, an R package with basic MCI and UMFI functions, as well as an upcoming Python package for UMFI can be found at `https://github.com/HydroML/UMFI`.

4.1 Experiments on Simulated Data

In the following subsections, we compare UMFI and MCI on simulated data. The data in all scenarios contains one response variable y, four explanatory features x_1, x_2, x_3, x_4, and 1000 randomly generated observations. Each study is repeated 100 times to test and ensure stability (Yu, 2013).

4.1.1 Nonlinear Interactions

Interaction effects are common in many scientific disciplines where assessing feature importance is prevalent, including hydrology (Janssen and Ameli, 2021; Addor et al., 2018; Le et al., 2022; Li and Ameli, 2022), genomics (Catav et al., 2021; Wang et al., 2021; Orlenko and Moore, 2021; Wright et al., 2016), and glaciology (Edwards et al., 2021; Bach et al., 2018; Brenning and Azócar, 2010; Sevestre and Benn, 2015). So, as was done in Catav et al. (2021), we assess the ability of MCI and UMFI to detect nonlinear interaction effects in the data (Marx et al., 2021). We consider:

$$x_1, x_2, x_3, x_4 \sim \mathcal{N}(0, 1)$$
$$y = x_1 + x_2 + sign(x_1 * x_2) + x_3 + x_4.$$

Feature importance metrics should ideally conclude that x_1 and x_2 have higher importance compared to x_3 and x_4 because of the extra interaction term, $sign(x_1 * x_2)$. Figure 1a shows consistently good performance across all methods. Each method gave high relative importance scores to x_1 and x_2, while x_3 and x_4 received less, but still substantial importance. All methods show similar variability.

4.1.2 Correlated Interactions

Interacting features are often correlated (Jakulin and Bratko, 2003; Janssen and Ameli, 2021). So, this simulation study aims to repeat the nonlinear interactions study, except now x_1 and x_2 are highly correlated with eachother. In the same way, x_3 and x_4 are highly correlated with eachother. Let $A, B, C, D, E, G \sim \mathcal{N}(0, 1)$. We consider:

$$x_1 = A + B,\ x_2 = B + C,\ x_3 = D + E,\ x_4 = E + G$$
$$y = x_1 + x_2 + sign(x_1 * x_2) + x_3 + x_4.$$

Just as with the interaction experiment with independent features, we would expect x_1 and x_2 to be more important than x_3 and x_4 because of the extra interaction term, $sign(x_1 * x_2)$. The results in Figure 1b show that UMFI provides substantially better feature importance scores compared to MCI when correlated interactions are present. MCI estimates that all features have approximately the same feature importance scores, while both UMFI methods appropriately give significantly greater importance to x_1 and x_2 compared with x_3 and x_4. MCI fails in this experiment because it penalizes feature subsets that share information with the feature of interest (Equation (2)). For example, if we are assessing the MCI score for x_1, since x_2 is strongly correlated with x_1, then the predictive power offered by x_1 on top of a subset S would be diminished by the presence of $x_2 \in S$. Therefore, x_2 is not utilized in the MCI score for x_1, which prevents the detection of the interaction term $sign(x_1 * x_2)$. UMFI is able to detect this interaction because it can extract the information from x_2 that interacts with x_1 while keeping this extracted feature independent of x_1. We suspect that similar results could be demonstrated in the presence of dependent, but uncorrelated interactions.

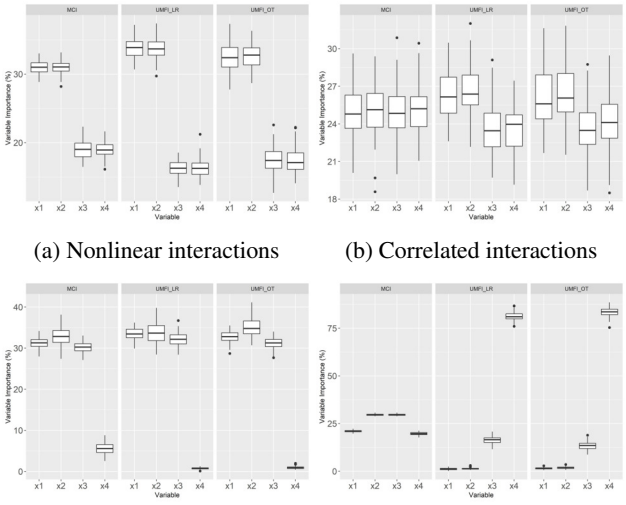

(a) Nonlinear interactions (b) Correlated interactions

(c) Correlation (d) Blood relation

Figure 1: Results for the experiments on simulated data from Subsection 4.1. Feature importance scores are shown as a percentage of the total for each of x_1 to x_4 from 100 replications. Results are shown for marginal contribution feature importance (MCI), ultra-marginal feature importance with linear regression (UMFI_LR), and ultra-marginal feature importance with pairwise optimal transport (UMFI_OT).

4.1.3 Correlation

Feature importance methods that seek to explain data should not change the measured importance of features in the presence of redundant variables according to the IRI axiom. To test this, we implement a simulation study sim-

ilar to the ones found in Catav et al. (2021). Let $\epsilon \sim \mathcal{N}(0, 0.01)$. We consider:

$$x_1, x_2, x_4 \sim \mathcal{N}(0, 1),\ x_3 = x_1 + \epsilon$$
$$y = x_1 + x_2.$$

The addition of x_3, which is approximately a duplicate of x_1, should not alter the importance of x_1, which should remain equally as important as x_2 since they have the same influence on the response y. The results shown in Figure 1c show that both MCI and UMFI work reasonably well. As with the previous simulation experiment, the variability is consistent across methods. As was desired, UMFI with linear regression shows approximately equal relative importance scores for x_1 and x_2. The importance given to x_2 was slightly greater than x_1 according to MCI and UMFI with optimal transport. Interestingly, MCI assigns some importance to x_4, which was independent of the response, while both UMFI methods assign importance scores close to zero. Because of this, we conclude that UMFI with linear regression performs the best in this simulated scenario.

4.1.4 Blood Relation

To ensure that UMFI is suitable for scientific inference, and that it could be used to learn part of the structure of causal graphs in theory as well as in practice, we implement the blood relation simulation experiment. In this study, data is generated from the causal graph in Figure 2, which was inspired by the collider causal graph found in Harel et al. (2022). The feature S is unobserved, thus x_3 and x_4 are the only observed features that are blood related to the response y. According to the blood relation axiom, x_3 and x_4 should be given high and positive importance while x_1 and x_2 should receive zero importance. In Section 3 and Supplement C, we prove that in ideal scenarios, UMFI will satisfy the blood relation axiom. We hypothesize that we can extend this to real-world scenarios where non-Gaussian features and interaction information appear. To test this, we consider:

$$\delta \sim \mathcal{U}(-1, 1),\ \gamma \sim Exp(1),\ \epsilon \sim \mathcal{U}(-0.5, 0.5)$$
$$x_1, S \sim \mathcal{N}(0, 1),\ x_2 = 3x_1 + \delta,\ x_3 = x_2 + S$$
$$y = S + \epsilon,\ x_4 = y + \gamma.$$

The results shown in Figure 1d indicate that MCI fails to distinguish the blood related features since more than half of the total importance is shared between $x_1, x_2 \notin BR(Y)$, while $x_3, x_4 \in BR(Y)$ together received less than half of the total importance. In contrast, UMFI_LR and UMFI_OT detect that x_1 and x_2 should have approximately zero importance while giving most of the importance to x_4 and the rest of the relative importance to x_3.

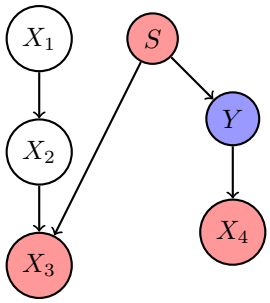

Figure 2: The full causal graph generating the data for the blood relation simulation experiment in Section 4.1.4. Blood related vertices to the response Y (blue) are coloured in red. S and X_4 are directly causally related to Y, whereas X_3 is related to Y via the common ancestor S.

4.2 BRCA Experiments

We use the same breast cancer (BRCA) classification dataset (Tomczak et al., 2015) used in previous feature importance studies including Catav et al. (2021) and Covert et al. (2020) to test the quality and robustness of UMFI on real data. The original data contains over $17,000$ genes and 571 anonymous patients with one of four types of breast cancer. We consider the same subset of 50 genes as in Catav et al. (2021) and Covert et al. (2020) for easier computation and result visualization. Of the 50 selected genes, 10 are known to be associated with breast cancer, while the other 40 genes are randomly sampled. This data was downloaded from the MCI GitHub page. In Catav et al. (2021) and Covert et al. (2020), these 40 randomly sampled genes are assumed to be unassociated with breast cancer. However, to ensure a more definitive ground truth, we also randomly permute the values of these 40 genes across their respective 571 observations to further reduce the chance that these genes have any association with breast cancer.

Quality is then measured with the true positive and true negative rates: the 10 BRCA associated genes should have some non-zero importance (positive), and the other 40 genes should have exactly zero importance (negative). These experiments were run 200 times on different seeds and with a different random sample of 500 patients for each iteration. Robustness is measured using the standardized interquartile range (SIQR) from the repeated experiments, which is calculated by dividing the average IQR across the 50 features by the average median. This experiment is too computationally intensive for MCI to be calculated exactly, so we implement MCI assuming soft 2-size submodularity (see the supplement of Catav et al. (2021) for details).

We found that MCI and UMFI (UMFI_LR and UMFI_OT) correctly gave significant importance to the 10 genes that are known to be associated with breast cancer (Figure 3). Interestingly, the order of important features was similar

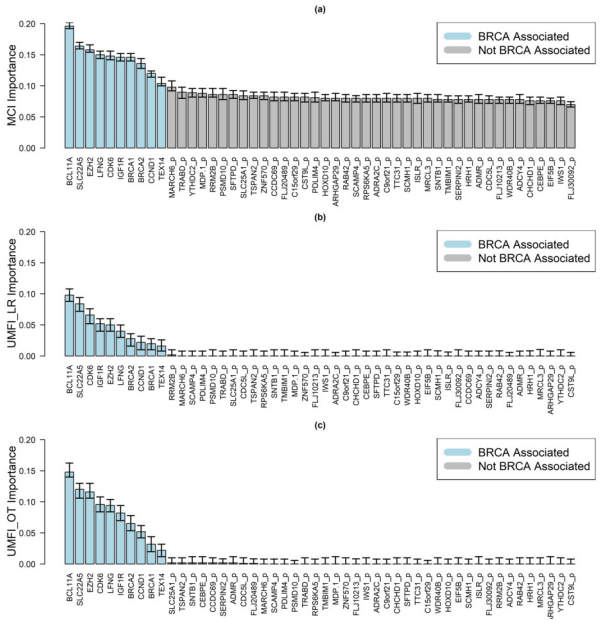

Figure 3: Median feature importance scores provided by (a) MCI, (b) UMFI with linear regression, and (c) UMFI with pairwise optimal transport, for each gene in the BRCA dataset after 200 iterations. Genes colored in blue are known to be associated with breast cancer while genes colored in grey are random permutations of randomly selected genes, which we assume to be unassociated with breast cancer. The first and third quantiles of the scores are visualized as error bars for each gene.

across methods, with BCL11A and SLC22A5 always ranking first, and TEX14 always being the least important of the 10 BRCA-associated genes. However, MCI consistently gives non-zero median importance to all features, while UMFI correctly gives zero median importance to the majority of the randomized genes. Furthermore, UMFI's performance in this experiment improves with increased iterations. After running the experiment 5000 times, both UMFI methods achieve perfect accuracy when distinguishing between important and permuted features (Supplement G.2.1). Although UMFI scores have higher variability than MCI (Table 1), Figure 3 shows that UMFI provides a more accurate and interpretable scoring, since it better separates the 10 associated genes from the 40 unassociated genes.

4.3 Computational Complexity

MCI must train and evaluate a model for each element of the power set of the feature set, which implies $O(2^p)$ model trainings if there are p features. If the evaluation function ν obeys soft k-size submodularity, then the maximizing subset has no more than k elements, which reduces the number of model trainings to $O(p^{k+1})$ (Catav et al., 2021). UMFI circumvents the exponential training time since it can be evaluated after $O(p)$ model trainings, though the extra step of dependency removal is required. To confirm the above statements, and to show that the extra model trainings required for MCI dominate the computation time for removing dependencies in UMFI, we ran a simple timed experiment. For a range of dataset sizes from the BRCA data, we evaluate the computation time for calculating the feature importance scores of all features using MCI and UMFI. We ran this experiment for a dataset with 5 features, and then slowly added features until our given time budget of 1 hour ran out. Once all 50 BRCA features were used, more features were randomly generated. All datasets had 571 observations. These experiments were run using an Intel Core i9-9980HK CPU 2.40GHz with 32GB of RAM. Code was parallelized in R, and 12 of the 16 available threads were used.

Table 1: The standardized interquartile range (SIQR), true positive rate (TPR), true negative rate (TNR), overall accuracy (OA), and the number of features for which feature importance can be calculated within 60 minutes are displayed after running the methods on the BRCA data.

Method	SIQR	TPR	TNR	OA	@1hr
MCI (k=2)	**6.6 %**	**1**	0	0.20	130
UMFI (LR)	41.9%	**1**	**0.975**	**0.98**	**4010**
UMFI (OT)	28.5%	**1**	0.775	0.82	3000

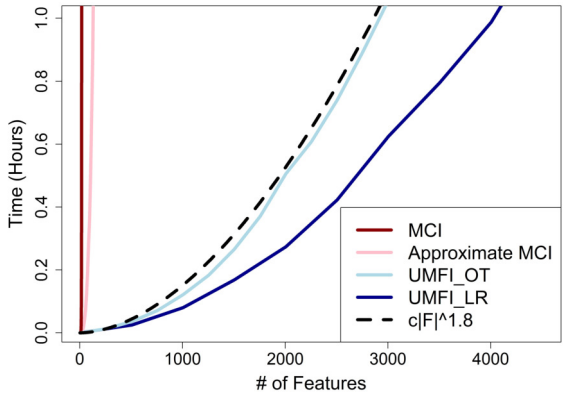

Figure 4: Computation time for a single iteration of each method including: MCI (dark red), MCI with the soft 2-size-submodularity assumption (pink), UMFI_OT (light blue), and UMFI_LR (dark blue), plotted against the number of processed features.

From Figure 4, we can observe that UMFI is approximately super-linear, with UMFI_OT incurring more computational cost compared to UMFI_LR. Giving each method one hour

to run, MCI processed 19 features, MCI with the soft 2-size submodularity assumption processed 130 features, UMFI_OT processed about 3000 features, and UMFI_LR processed about 4000 features (Table 1).

5 CONCLUSION

In this study, we introduced three ideal axioms that feature importance measures should satisfy if they claim to be useful for learning from data. We then introduced ultra-marginal feature importance (UMFI), a new method that uses preprocessing techniques, originally developed in the domain of AI fairness, to provide fast and accurate feature importance scores for the purpose of explaining data. We proved that UMFI satisfies all three of the introduced axioms under certain assumptions. When compared with MCI, experimental results showed that UMFI, implemented with linear regression and optimal transport as preprocessing techniques, was able to provide more accurate estimates of feature importance on real and simulated data, particularly in the presence of correlated interactions and unrelated features. Supplement G shows that UMFI also compares favourably against other baseline methods including permutation importance, conditional permutation importance, and ablation.

Throughout the work on this paper, several shortcomings appeared. First, we only considered two simple methods for removing dependencies, linear regression and pairwise optimal transport. Other methods certainly exist in the literature, including optimal transport with chaining (Johndrow and Lum, 2019), neural networks (Calmon et al., 2017; Song et al., 2019), or principal inertial components (Wang et al., 2019). Though our two methods performed fairly well on the real and simulated datasets in Section 4, optimal transport and linear regression failed to find representations of the data that were independent of the protected attribute when we tested the methods on a hydrology dataset with more shared information compared to BRCA (Addor et al., 2017) (Supplement G.4). However, neural nets, principal inertial components, or implementing optimal transport with better estimates of the conditional CDF certainly could have given better results. Although dependencies were not removed optimally for the hydrology dataset, the importance scores were still reasonably accurate. Second, UMFI scores are less robust than MCI since they have higher variability, however, because of the significantly lower computational cost, UMFI can be run multiple times and averaged to increase robustness and compute confidence intervals. Third, it is not clear how closely random forests or other measures of multivariate dependence can approximate the universal predictive power ν and mutual information in practice. In the same vein, it is unclear if multivariate measures of dependence usually satisfy properties such as monotonicity, redundancy invariance, and supermodularity, which we used UMFI's adherence to our proposed axioms. Finally, though UMFI can work for any arbitrary feature type, in this paper, we have only considered datasets with continuous explanatory variables.

In future work, we would like to test how well other methods, such as neural networks, pair with UMFI while further testing on a wider variety of variable types (i.e., binary, categorical, and ordinal). We also believe that exploring the effectiveness of dependency removal techniques is worthwhile in its own right. We would also like to test how well UMFI scales to large datasets. In these settings, UMFI would benefit from a fast algorithm for computing confidence intervals and p-values to counteract its variability. Comparing different measures of multivariate dependence in their ability to approximate universal predictive power and satisfy common assumptions such as monotonicity would also be of interest to the broader feature importance community. Currently, UMFI is limited to providing a single measure of global variable importance. Extending our methods such that UMFI can be decomposed into different orders of interaction effects or redundant information in a similar way to functional ANOVA (Lengerich et al., 2020; Märtens and Yau, 2020; Hooker, 2007; Huang, 1998; Stone, 1994), commonality analysis (Amado, 1999; Daube et al., 2019; Seibold and McPHEE, 1979; Stoffel et al., 2021; Ray-Mukherjee et al., 2014), partial information decomposition (Rosas et al., 2020; Varley, 2023; Gutknecht et al., 2021; Mediano et al., 2022; Kolchinsky, 2022; Suzuki et al., 2022; Goodwell and Bassiouni, 2022; Goodwell et al., 2020; Gurushankar et al., 2022; Wollstadt et al., 2021), or functional decomposition (Bordt and von Luxburg, 2022; Hiabu et al., 2022) could provide interesting future research directions.

To reiterate, UMFI is a powerful tool for detecting and explaining the relationships hidden within observational data. We emphasise that UMFI is just a framework. A variety of other methods can be used to estimate the universal predictive power ν including, but not limited to, XGBoost, neural networks, QMD, or FOCI (Griessenberger et al., 2022; Azadkia and Chatterjee, 2021). Furthermore, new preprocessing techniques for dependence removal are still being developed in the AI fairness community, so these, in addition to other existing methods, can be used in future applications of UMFI for additional improvements. We hope that UMFI will be a useful tool for learning from data in a variety of disciplines including bioinfomatics, earth sciences, psychology, and health science.

Acknowledgements

We thank Dr. Ali A. Ameli for his support and motivation during this process. We thank all of the authors of the papers we cited, especially Dr. Chandra Nair for his help with concepts in information theory and Boyang Fu for his experimental advice.

References

Addor, N., Nearing, G., Prieto, C., Newman, A., Le Vine, N., and Clark, M. P. (2018). A ranking of hydrological signatures based on their predictability in space. *Water Resources Research*, 54(11):8792–8812.

Addor, N., Newman, A. J., Mizukami, N., and Clark, M. P. (2017). The camels data set: catchment attributes and meteorology for large-sample studies. *Hydrology and Earth System Sciences*, 21(10):5293–5313.

Al-Ani, A., Deriche, M., and Chebil, J. (2003). A new mutual information based measure for feature selection. *Intelligent Data Analysis*, 7(1):43–57.

Amado, A. J. (1999). Partitioning predicted variance into constituent parts: A primer on regression commonality analysis.

Apley, D. W. and Zhu, J. (2020). Visualizing the effects of predictor variables in black box supervised learning models. *Journal of the Royal Statistical Society: Series B (Statistical Methodology)*, 82(4):1059–1086.

Azadkia, M. and Chatterjee, S. (2021). A simple measure of conditional dependence. *The Annals of Statistics*, 49(6):3070–3102.

Bach, E., Radić, V., and Schoof, C. (2018). How sensitive are mountain glaciers to climate change? insights from a block model. *Journal of Glaciology*, 64(244):247–258.

Battiti, R. (1994). Using mutual information for selecting features in supervised neural net learning. *IEEE Transactions on neural networks*, 5(4):537–550.

Bazaga, A., Leggate, D., and Weisser, H. (2020). Genome-wide investigation of gene-cancer associations for the prediction of novel therapeutic targets in oncology. *Scientific reports*, 10(1):1–10.

Bénard, C., Biau, G., Da Veiga, S., and Scornet, E. (2022). Shaff: Fast and consistent shapley effect estimates via random forests. In *International Conference on Artificial Intelligence and Statistics*, pages 5563–5582. PMLR.

Bennasar, M., Hicks, Y., and Setchi, R. (2015). Feature selection using joint mutual information maximisation. *Expert Systems with Applications*, 42(22):8520–8532.

Bi, J. (2012). A review of statistical methods for determination of relative importance of correlated predictors and identification of drivers of consumer liking. *Journal of Sensory Studies*, 27(2):87–101.

Bird, S., Dudík, M., Edgar, R., Horn, B., Lutz, R., Milan, V., Sameki, M., Wallach, H., and Walker, K. (2020). Fairlearn: A toolkit for assessing and improving fairness in ai. *Microsoft, Tech. Rep. MSR-TR-2020-32*.

Bordt, S. and von Luxburg, U. (2022). From shapley values to generalized additive models and back. *arXiv preprint arXiv:2209.04012*.

Breiman, L. (2001). Random forests. *Machine learning*, 45(1):5–32.

Breiman, L., Friedman, J. H., Olshen, R. A., and Stone, C. J. (2017). *Classification and regression trees*. Routledge.

Brenning, A. and Azócar, G. (2010). Statistical analysis of topographic and climatic controls and multispectral signatures of rock glaciers in the dry andes, chile (27–33 s). *Permafrost and Periglacial Processes*, 21(1):54–66.

Calmon, F., Wei, D., Vinzamuri, B., Natesan Ramamurthy, K., and Varshney, K. R. (2017). Optimized preprocessing for discrimination prevention. *Advances in neural information processing systems*, 30.

Catav, A., Fu, B., Ernst, J., Sankararaman, S., and Gilad-Bachrach, R. (2020). Marginal contribution feature importance–an axiomatic approach for the natural case. *arXiv preprint arXiv:2010.07910*.

Catav, A., Fu, B., Zoabi, Y., Meilik, A. L. W., Shomron, N., Ernst, J., Sankararaman, S., and Gilad-Bachrach, R. (2021). Marginal contribution feature importance - an axiomatic approach for explaining data. In Meila, M. and Zhang, T., editors, *Proceedings of the 38th International Conference on Machine Learning*, volume 139 of *Proceedings of Machine Learning Research*, pages 1324–1335. PMLR.

Chen, H., Janizek, J. D., Lundberg, S., and Lee, S.-I. (2020). True to the model or true to the data? *arXiv preprint arXiv:2006.16234*.

Chen, T., He, T., Benesty, M., Khotilovich, V., Tang, Y., Cho, H., Chen, K., et al. (2015). Xgboost: extreme gradient boosting. *R package version 0.4-2*, 1(4):1–4.

Cohen, S., Dror, G., and Ruppin, E. (2007). Feature selection via coalitional game theory. *Neural Computation*, 19(7):1939–1961.

Consortium, W. T. C. C. et al. (2007). Genome-wide association study of 14,000 cases of seven common diseases and 3,000 shared controls. *Nature*, 447(7145):661.

Cover, T. M. and Thomas, J. A. (2006). *Elements of Information Theory 2nd Edition (Wiley Series in Telecommunications and Signal Processing)*. Wiley-Interscience.

Covert, I., Lundberg, S. M., and Lee, S.-I. (2020). Understanding global feature contributions with additive importance measures. *Advances in Neural Information Processing Systems*, 33:17212–17223.

Covert, I., Lundberg, S. M., and Lee, S.-I. (2021). Explaining by removing: A unified framework for model explanation. *J. Mach. Learn. Res.*, 22:209–1.

Darlington, R. B. (1968). Multiple regression in psychological research and practice. *Psychological bulletin*, 69(3):161.

Daube, C., Giordano, B., Schyns, P. G., and Ince, R. A. (2019). Quantitatively comparing predictive models with the partial information decomposition.

Dawid, A. P. (1979). Conditional independence in statistical theory. *Journal of the Royal Statistical Society: Series B (Methodological)*, 41(1):1–15.

Debeer, D., Hothorn, T., Strobl, C., and Debeer, M. D. (2021). Package 'permimp'.

Debeer, D. and Strobl, C. (2020). Conditional permutation importance revisited. *BMC bioinformatics*, 21(1):1–30.

DelSole, T. and Tippett, M. K. (2007). Predictability: Recent insights from information theory. *Reviews of Geophysics*, 45(4).

Easton, D. F., Pooley, K. A., Dunning, A. M., Pharoah, P. D., Thompson, D., Ballinger, D. G., Struewing, J. P., Morrison, J., Field, H., Luben, R., et al. (2007). Genome-wide association study identifies novel breast cancer susceptibility loci. *Nature*, 447(7148):1087–1093.

Edwards, T. L., Nowicki, S., Marzeion, B., Hock, R., Goelzer, H., Seroussi, H., Jourdain, N. C., Slater, D. A., Turner, F. E., Smith, C. J., et al. (2021). Projected land ice contributions to twenty-first-century sea level rise. *Nature*, 593(7857):74–82.

Fan, J. and Lv, J. (2008). Sure independence screening for ultrahigh dimensional feature space. *Journal of the Royal Statistical Society: Series B (Statistical Methodology)*, 70(5):849–911.

Freiesleben, T., König, G., Molnar, C., and Tejero-Cantero, A. (2022). Scientific inference with interpretable machine learning: Analyzing models to learn about real-world phenomena. *arXiv preprint arXiv:2206.05487*.

Galton, F. (1889). I. co-relations and their measurement, chiefly from anthropometric data. *Proceedings of the Royal Society of London*, 45(273-279):135–145.

Geurts, P., Ernst, D., and Wehenkel, L. (2006). Extremely randomized trees. *Machine learning*, 63(1):3–42.

Gibson, W. (1962). Orthogonal predictors: A possible resolution of the hoffman-ward controversy. *Psychological reports*, 11(1):32–34.

Gill, D. A., Mascia, M. B., Ahmadia, G. N., Glew, L., Lester, S. E., Barnes, M., Craigie, I., Darling, E. S., Free, C. M., Geldmann, J., et al. (2017). Capacity shortfalls hinder the performance of marine protected areas globally. *Nature*, 543(7647):665–669.

Gitiaux, X. and Rangwala, H. (2021a). Fair representations by compression. In *Proceedings of the AAAI Conference on Artificial Intelligence*, volume 35, pages 11506–11515.

Gitiaux, X. and Rangwala, H. (2021b). Learning smooth and fair representations. In *International conference on artificial intelligence and statistics*, pages 253–261. PMLR.

Gitiaux, X. and Rangwala, H. (2022). Sofair: Single shot fair representation learning. *arXiv preprint arXiv:2204.12556*.

Gong, W., Gupta, H. V., Yang, D., Sricharan, K., and Hero III, A. O. (2013). Estimating epistemic and aleatory uncertainties during hydrologic modeling: An information theoretic approach. *Water resources research*, 49(4):2253–2273.

Goodwell, A. E. and Bassiouni, M. (2022). Source relationships and model structures determine information flow paths in ecohydrologic models. *Water Resources Research*, 58(9):e2021WR031164.

Goodwell, A. E., Jiang, P., Ruddell, B. L., and Kumar, P. (2020). Debates—does information theory provide a new paradigm for earth science? causality, interaction, and feedback. *Water Resources Research*, 56(2):e2019WR024940.

Greenland, S., Pearl, J., and Robins, J. M. (1999). Causal diagrams for epidemiologic research. *Epidemiology*, pages 37–48.

Griessenberger, F., Junker, R. R., and Trutschnig, W. (2022). On a multivariate copula-based dependence measure and its estimation. *Electronic Journal of Statistics*, 16(1):2206–2251.

Griffith, V. and Koch, C. (2014). Quantifying synergistic mutual information. *Guided self-organization: inception*, pages 159–190.

Grömping, U. (2009). Variable importance assessment in regression: linear regression versus random forest. *The American Statistician*, 63(4):308–319.

Gurushankar, K., Venkatesh, P., and Grover, P. (2022). Extracting unique information through markov relations. In *2022 58th Annual Allerton Conference on Communication, Control, and Computing (Allerton)*, pages 1–6. IEEE.

Gutknecht, A. J., Wibral, M., and Makkeh, A. (2021). Bits and pieces: Understanding information decomposition from part-whole relationships and formal logic. *Proceedings of the Royal Society A*, 477(2251):20210110.

Harder, M., Salge, C., and Polani, D. (2013). Bivariate measure of redundant information. *Physical Review E*, 87(1):012130.

Harel, N., Gilad-Bachrach, R., and Obolski, U. (2022). Inherent inconsistencies of feature importance. *arXiv preprint arXiv:2206.08204*.

Hiabu, M., Meyer, J. T., and Wright, M. N. (2022). Unifying local and global model explanations by functional decomposition of low dimensional structures. *arXiv preprint arXiv:2208.06151*.

Hooker, G. (2007). Generalized functional anova diagnostics for high-dimensional functions of dependent variables. *Journal of Computational and Graphical Statistics*, 16(3):709–732.

Hooker, G., Mentch, L., and Zhou, S. (2021). Unrestricted permutation forces extrapolation: variable importance requires at least one more model, or there is no free variable importance. *Statistics and Computing*, 31(6):1–16.

Huang, J. Z. (1998). Projection estimation in multiple regression with application to functional anova models. *The annals of statistics*, 26(1):242–272.

Jakulin, A. and Bratko, I. (2003). Quantifying and visualizing attribute interactions: An approach based on entropy.

Janssen, A., Hoogendoorn, M., Cnossen, M. H., Mathôt, R. A., Group, O.-C. S., Consortium, S., Cnossen, M., Reitsma, S., Leebeek, F., Mathôt, R., Fijnvandraat, K., et al. (2022). Application of shap values for inferring the optimal functional form of covariates in pharmacokinetic modeling. *CPT: Pharmacometrics & Systems Pharmacology*.

Janssen, J. and Ameli, A. A. (2021). A hydrologic functional approach for improving large-sample hydrology performance in poorly gauged regions. *Water Resources Research*, 57(9):e2021WR030263.

Jehn, F. U., Bestian, K., Breuer, L., Kraft, P., and Houska, T. (2020). Using hydrological and climatic catchment clusters to explore drivers of catchment behavior. *Hydrology and Earth System Sciences*, 24(3):1081–1100.

Johndrow, J. E. and Lum, K. (2019). An algorithm for removing sensitive information: application to race-independent recidivism prediction. *The Annals of Applied Statistics*, 13(1):189–220.

Johnsen, P. V., Riemer-Sørensen, S., DeWan, A. T., Cahill, M. E., and Langaas, M. (2021). A new method for exploring gene–gene and gene–environment interactions in gwas with tree ensemble methods and shap values. *BMC bioinformatics*, 22(1):1–29.

Kang, C. and Tian, J. (2009). Markov properties for linear causal models with correlated errors. *Journal of Machine Learning Research*, 10(1).

Kinney, J. B. and Atwal, G. S. (2014). Equitability, mutual information, and the maximal information coefficient. *Proceedings of the National Academy of Sciences*, 111(9):3354–3359.

Kolchinsky, A. (2022). A novel approach to the partial information decomposition. *Entropy*, 24(3):403.

König, G., Freiesleben, T., Bischl, B., Casalicchio, G., and Grosse-Wentrup, M. (2021). Decomposition of global feature importance into direct and associative components (dedact). *arXiv preprint arXiv:2106.08086*.

Kraskov, A., Stögbauer, H., and Grassberger, P. (2004). Estimating mutual information. *Physical review E*, 69(6):066138.

Kruskal, W. (1984). Concepts of relative importance. *Qüestiió. 1984, vol. 8, núm. 1*.

Lau, K., Nair, C., and Ng, D. (2022). A mutual information inequality and some applications. In *2022 IEEE International Symposium on Information Theory (ISIT)*, pages 951–956. IEEE.

Lauritzen, S. and Sadeghi, K. (2018). Unifying markov properties for graphical models. *The Annals of Statistics*, 46(5):2251–2278.

Le, E., Ameli, A., Janssen, J., and Hammond, J. (2022). Snow persistence explains stream high flow and low flow signatures with differing relationships by aridity and climatic seasonality. *Hydrology and Earth System Sciences Discussions*, pages 1–22.

Lengerich, B., Tan, S., Chang, C.-H., Hooker, G., and Caruana, R. (2020). Purifying interaction effects with the functional anova: An efficient algorithm for recovering identifiable additive models. In *International Conference on Artificial Intelligence and Statistics*, pages 2402–2412. PMLR.

Li, H. and Ameli, A. (2022). A statistical approach for identifying factors governing streamflow recession behaviour. *Hydrological Processes*, 36(10):e14718.

Liaw, A., Wiener, M., et al. (2002). Classification and regression by randomforest. *R news*, 2(3):18–22.

Louppe, G., Wehenkel, L., Sutera, A., and Geurts, P. (2013). Understanding variable importances in forests of randomized trees. *Advances in neural information processing systems*, 26.

Lundberg, S. M. and Lee, S.-I. (2017). A unified approach to interpreting model predictions. *Advances in neural information processing systems*, 30.

Malouche, D. and Sevestre-Ghalila, S. (2008). Estimating high dimensional faithful gaussian graphical models by low-order conditioning. In *Proceeding, of 26th IASTED International Multi-Conference on Applied Informatics, Artificial Intelligence and Applications*, pages 595–025.

Märtens, K. and Yau, C. (2020). Neural decomposition: Functional anova with variational autoencoders. In *International Conference on Artificial Intelligence and Statistics*, pages 2917–2927. PMLR.

Marx, A., Gretton, A., and Mooij, J. M. (2021). A weaker faithfulness assumption based on triple interactions. In *Uncertainty in Artificial Intelligence*, pages 451–460. PMLR.

Marx, C., Park, Y., Hasson, H., Wang, Y. B., Ermon, S., and Huan, J. (2022). But are you sure? an uncertainty-aware perspective on explainable ai.

Matthijs, Warmerdam, V., and ManyOthers (2019). scikit-fairness. `scikit-fairness.https://github.com/koaning/scikit-fairness`.

Mediano, P. A., Rosas, F. E., Luppi, A. I., Jensen, H. J., Seth, A. K., Barrett, A. B., Carhart-Harris, R. L., and Bor, D. (2022). Greater than the parts: a review of the information decomposition approach to causal emergence. *Philosophical Transactions of the Royal Society A*, 380(2227):20210246.

Molnar, C. (2020). *Interpretable machine learning*. Lulu. com.

Molnar, C., Freiesleben, T., König, G., Casalicchio, G., Wright, M. N., and Bischl, B. (2021). Relating the partial dependence plot and permutation feature importance to the data generating process. *arXiv preprint arXiv:2109.01433*.

Moyer, D., Gao, S., Brekelmans, R., Galstyan, A., and Ver Steeg, G. (2018). Invariant representations without adversarial training. *Advances in Neural Information Processing Systems*, 31.

Orlenko, A. and Moore, J. H. (2021). A comparison of methods for interpreting random forest models of genetic association in the presence of non-additive interactions. *BioData mining*, 14(1):1–17.

Probst, P., Boulesteix, A.-L., and Bischl, B. (2019). Tunability: importance of hyperparameters of machine learning algorithms. *The Journal of Machine Learning Research*, 20(1):1934–1965.

Ray-Mukherjee, J., Nimon, K., Mukherjee, S., Morris, D. W., Slotow, R., and Hamer, M. (2014). Using commonality analysis in multiple regressions: a tool to decompose regression effects in the face of multicollinearity. *Methods in Ecology and Evolution*, 5(4):320–328.

Reisach, A., Seiler, C., and Weichwald, S. (2021). Beware of the simulated dag! causal discovery benchmarks may be easy to game. *Advances in Neural Information Processing Systems*, 34:27772–27784.

Rosas, F. E., Mediano, P. A., Jensen, H. J., Seth, A. K., Barrett, A. B., Carhart-Harris, R. L., and Bor, D. (2020). Reconciling emergences: An information-theoretic approach to identify causal emergence in multivariate data. *PLoS computational biology*, 16(12):e1008289.

Schellhas, D., Neupane, B., Thammineni, D., Kanumuri, B., and Green, R. C. (2020). Distance correlation sure independence screening for accelerated feature selection in parkinson's disease vocal data. In *2020 International Conference on Computational Science and Computational Intelligence (CSCI)*, pages 1433–1438. IEEE.

Schmidt, L., Heße, F., Attinger, S., and Kumar, R. (2020). Challenges in applying machine learning models for hydrological inference: A case study for flooding events across germany. *Water Resources Research*, 56(5):e2019WR025924.

Seibold, D. R. and McPHEE, R. D. (1979). Commonality analysis: A method for decomposing explained variance in multiple regression analyses. *Human Communication Research*, 5(4):355–365.

Sevestre, H. and Benn, D. I. (2015). Climatic and geometric controls on the global distribution of surge-type glaciers: implications for a unifying model of surging. *Journal of Glaciology*, 61(228):646–662.

Shapley, L. S. (1953). A value for n-person games, contributions to the theory of games, 2, 307–317.

Shpitser, I. and Pearl, J. (2008). Complete identification methods for the causal hierarchy. *Journal of Machine Learning Research*, 9:1941–1979.

Soleymani, A., Raj, A., Bauer, S., Schölkopf, B., and Besserve, M. (2022). Causal feature selection via orthogonal search. *Transactions on Machine Learning Research*.

Song, J., Kalluri, P., Grover, A., Zhao, S., and Ermon, S. (2019). Learning controllable fair representations. In *The 22nd International Conference on Artificial Intelligence and Statistics*, pages 2164–2173. PMLR.

Spearman, C. (1961). " general intelligence" objectively determined and measured.

Stein, L., Clark, M. P., Knoben, W. J., Pianosi, F., and Woods, R. A. (2021). How do climate and catchment attributes influence flood generating processes? a large-sample study for 671 catchments across the contiguous usa. *Water Resources Research*, 57(4):e2020WR028300.

Steudel, B. and Ay, N. (2015). Information-theoretic inference of common ancestors. *Entropy*, 17(4):2304–2327.

Stoffel, M. A., Nakagawa, S., and Schielzeth, H. (2021). partr2: partitioning r2 in generalized linear mixed models. *PeerJ*, 9:e11414.

Stone, C. J. (1994). The use of polynomial splines and their tensor products in multivariate function estimation. *The annals of statistics*, 22(1):118–171.

Sun, S., Dong, B., and Zou, Q. (2021). Revisiting genome-wide association studies from statistical modelling to machine learning. *Briefings in Bioinformatics*, 22(4):bbaa263.

Sutera, A., Louppe, G., Huynh-Thu, V. A., Wehenkel, L., and Geurts, P. (2021). From global to local mdi variable importances for random forests and when they are shapley values. *Advances in Neural Information Processing Systems*, 34.

Suzuki, K., Matsuzaki, S.-i. S., and Masuya, H. (2022). Decomposing predictability to identify dominant causal drivers in complex ecosystems. *Proceedings of the National Academy of Sciences*, 119(42):e2204405119.

Tan, Z., Yeom, S., Fredrikson, M., and Talwalkar, A. (2020). Learning fair representations for kernel models. In *International Conference on Artificial Intelligence and Statistics*, pages 155–166. PMLR.

Taufiq, M. F., Blöbaum, P., and Minorics, L. (2023). Manifold restricted interventional shapley values. *arXiv preprint arXiv:2301.04041*.

Tolo̧si, L. and Lengauer, T. (2011). Classification with correlated features: unreliability of feature ranking and solutions. *Bioinformatics*, 27(14):1986–1994.

Tomczak, K., Czerwińska, P., and Wiznerowicz, M. (2015). The cancer genome atlas (tcga): an immeasurable source of knowledge. *Contemporary oncology*, 19(1A):A68.

Varley, T. F. (2023). Flickering emergences: The question of locality in information-theoretic approaches to emergence. *Entropy*, 25(1):54.

Vowels, M. J., Camgoz, N. C., and Bowden, R. (2021). D'ya like dags? a survey on structure learning and causal discovery. *ACM Computing Surveys (CSUR)*.

Wang, H., Bennett, D. A., De Jager, P. L., Zhang, Q.-Y., and Zhang, H.-Y. (2021). Genome-wide epistasis analysis for alzheimer's disease and implications for genetic risk prediction. *Alzheimer's research & therapy*, 13(1):1–13.

Wang, H. and Calmon, F. P. (2017). An estimation-theoretic view of privacy. In *2017 55th Annual Allerton Conference on Communication, Control, and Computing (Allerton)*, pages 886–893. IEEE.

Wang, H., Vo, L., Calmon, F. P., Médard, M., Duffy, K. R., and Varia, M. (2019). Privacy with estimation guarantees. *IEEE Transactions on Information Theory*, 65(12):8025–8042.

Williams, P. L. and Beer, R. D. (2010). Nonnegative decomposition of multivariate information. *arXiv preprint arXiv:1004.2515*.

Williams, T. C., Bach, C. C., Matthiesen, N. B., Henriksen, T. B., and Gagliardi, L. (2018). Directed acyclic graphs: a tool for causal studies in paediatrics. *Pediatric research*, 84(4):487–493.

Williamson, B. and Feng, J. (2020). Efficient nonparametric statistical inference on population feature importance using shapley values. In *International Conference on Machine Learning*, pages 10282–10291. PMLR.

Wollstadt, P., Schmitt, S., and Wibral, M. (2021). A rigorous information-theoretic definition of redundancy and relevancy in feature selection based on (partial) information decomposition. *arXiv preprint arXiv:2105.04187*.

Wright, M. N. and Ziegler, A. (2015). ranger: A fast implementation of random forests for high dimensional data in c++ and r. *arXiv preprint arXiv:1508.04409*.

Wright, M. N., Ziegler, A., and König, I. R. (2016). Do little interactions get lost in dark random forests? *BMC bioinformatics*, 17:1–10.

Wright, S. (1921). Correlation and causation.

Wurm, L. H. and Fisicaro, S. A. (2014). What residualizing predictors in regression analyses does (and what it does not do). *Journal of memory and language*, 72:37–48.

Yang, J.-B. and Ong, C.-J. (2012). An effective feature selection method via mutual information estimation. *IEEE Transactions on Systems, Man, and Cybernetics, Part B (Cybernetics)*, 42(6):1550–1559.

Yeung, R. W. (2002). *A first course in information theory*. Springer Science & Business Media.

Yu, B. (2013). Stability. *Bernoulli*, 19(4):1484–1500.

Yu, K., Liu, L., Li, J., and Chen, H. (2018). Mining markov blankets without causal sufficiency. *IEEE transactions on neural networks and learning systems*, 29(12):6333–6347.

A Mutual information

A.1 Properties of mutual information

Theorem A.1 (Symmetry of conditional mutual information (Yeung, 2002))**.**

$$I(Y;X|Z) = I(X;Y|Z)$$

Theorem A.2 (Chain rule for mutual information (Yeung, 2002))**.**

$$I(Y;X,Z) = I(Y;Z) + I(Y;X|Z) = I(Y;X) + I(Y;Z|X)$$

Theorem A.3 (Supermodularity under independence)**.** *Let S, X_1, X_2 be random variables such that $X_1 \perp\!\!\!\perp (S, X_2)$. Then, $I(Y;S,X_1,X_2) - I(Y;S,X_2) \geq I(Y;S,X_1) - I(Y;S)$ (Lau et al., 2022; Steudel and Ay, 2015).*

Proof.

$$\begin{aligned}
&I(Y;S,X_1,X_2) - I(Y;S,X_2)\\
&= I(Y;S,X_2) + I(Y;X_1|S,X_2) - I(Y;S,X_2) \quad \text{(by chain rule)}\\
&= I(Y;X_1|S,X_2) = I(X_1;Y|S,X_2) \quad \text{(by symmetry)}\\
&= I(X_1;Y,S,X_2) - I(X_1;S,X_2) \quad \text{(by chain rule)}\\
&= I(X_1;Y,S,X_2) = I(Y,S,X_2;X_1) \quad \text{(by } X_1 \perp\!\!\!\perp (S,X_2) \text{ and symmetry)}\\
&\geq I(Y,S;X_1) = I(X_1;Y,S) \quad \text{(by monotonicity of mutual information and symmetry)}\\
&= I(X_1;Y|S) = I(Y;X_1|S) \quad \text{(by chain rule, } X_1 \perp\!\!\!\perp S \text{, and symmetry)}\\
&= I(Y;S,X_1) - I(Y;S) \quad \text{(by chain rule)}
\end{aligned}$$

□

Theorem A.4 (Data processing inequality)**.** *Let X, Y, Z be three random variables forming a Markov chain $X \to Y \to Z$, i.e. $X \perp\!\!\!\perp Z|Y$. Then, $I(X;Y) \geq I(X;Z)$.*

Proof. The proof can be found in Cover and Thomas (2006, p. 32). □

Theorem A.5. *Let F be a set of features used to predict the response Y. Then $I(Y;F) \geq I(Y;g(F))$ for any deterministic function g. If g is injective, then $I(Y;F) = I(Y;g(F))$.*

Proof. The first claim $I(Y;F) \geq I(Y;g(F))$ follows from the data processing inequality (Theorem A.4) since $Y \to F \to g(F)$ forms a Markov chain.

If g is injective, then we may write $F = h(g(F))$ where $h : Im(g) \to F$ is the inverse of g restricted to the image of g. By the data processing inequality and the fact that $Y \perp\!\!\!\perp h(g(F))|g(F)$ we know that $I(Y;g(F)) \geq I(Y;h(g(F)))$. Then by the definition of h and g, we know that $I(Y;h(g(F))) = I(Y;F)$, thus $I(Y;g(F)) \geq I(Y;F)$. Combining with $I(Y;F) \geq I(Y;g(F))$ yields the desired claim, $I(Y;g(F)) = I(Y;F)$ when g is injective. □

A.2 Mutual information and feature importance

Let $F = \{x_1, ..., x_p\}$ be a set of features used to predict Y. As shown in Griffith and Koch (2014), the mutual information $I(Y;F) = I(Y;X_1, ..., X_p)$ can be visualized using a partial information (PI) diagram (Williams and Beer, 2010). We may interpret the mutual information shared between Y and F as a collection of non-negative pieces of information, whose sum forms $I(Y;F)$. Each of these pieces of information can be classified as unique, redundant, or synergistic (Figure 5). Unique information is the information about Y that comes from only one feature and nowhere else. Redundant information is information about Y that comes from a single feature, but which can also be found elsewhere in F. Synergistic information is information about Y that cannot be extracted from a single feature, but is available when multiple features are considered.

We note that the distinction between feature importance methods that seek to explain data versus methods that seek to explain or optimize a model comes from their treatment of redundant information (Wollstadt et al., 2021). Methods for explaining data, such as MCI or UMFI, aim to count all of the redundant information pertaining to X_i in $I(Y;F)$ towards the feature importance of x_i. Indeed, even though this information can be found elsewhere by a model, redundant information still constitutes part of the information that X_i shares about Y in the data. Conversely, a method mainly made for feature selection, such as conditional permutation importance (CPI), aims to count none of the redundant information towards the evaluation of a feature's importance, since this information is already found in another feature.

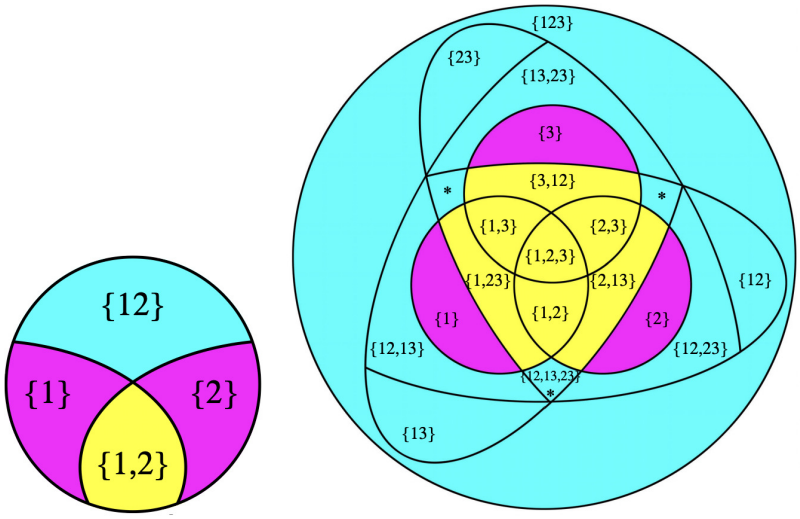

(a) $n = 2$ (b) $n = 3$

Figure 5: PI-diagrams taken from Griffith and Koch (2014) for $I(Y;F)$ when $|F| = 2$ (left) and $|F| = 3$ (right). Magenta represents unique information, redundant information is colored with yellow, and synergistic information is in cyan. The starred regions represent a single region.

Mutual information itself is a common choice in the context of feature selection (Battiti, 1994; Al-Ani et al., 2003; Yang and Ong, 2012; Bennasar et al., 2015). However, due to the computational cost and the limited number of observations available for the calculation of the high-dimensional joint probability density function, it is not practical to compute $I(Y;S)$. For feature selection, users are only interested in the importance given to the top k features. Therefore, mutual information-based feature selection methods typically bypass the computation of $I(Y;S)$ by instead studying the mutual information between the candidate feature and the response along with the mutual information between the candidate and the previously selected features (Bennasar et al., 2015; Battiti, 1994). These methods are much less suitable for feature importance when the goal is to explain the data since interactions cannot be considered, which is why the most common approach is to train machine learning models to determine an approximation of the universal predictive power (Catav et al., 2021; Chen et al., 2020; Covert et al., 2020; Williamson and Feng, 2020).

Another connection between feature importance and mutual information comes from Louppe et al. (2013), who showed that when extremely randomized trees' mean decrease in impurity (MDI) is used as a feature importance score, the MDI of a single feature converges to a weighted sum of conditional mutual information as the number of trees and the number of observations goes to infinity (Louppe et al., 2013). Also, the sum of the MDI scores across the feature set F converges to $I(Y;F)$.

A.3 Mutual information and machine learning evaluation functions

The evaluation function for a machine learning model $\nu_f(S)$ measures how well the response Y can be predicted using the model f given the information subset $S \in \mathcal{I}(F)$. Intuitively, the predictability or best possible accuracy $\nu_f(S)$ should ideally mirror or at least covary with the mutual information $I(Y;S)$ (DelSole and Tippett, 2007; Gong et al., 2013). While entropy and mutual information are usually examined in discrete settings, the continuous entropy and mutual information are linearly related to the analogous discretized version (Gong et al., 2013). In the case of regression, one can also closely relate mutual information to the explained variance of a model. Indeed, with some assumptions, mutual information and

R^2 accuracy are related. If we assume the response and predictions are jointly Gaussian and the predictions are unbiased (Cover and Thomas, 2006), we can approximate the mutual information between Y and F as:

$$I(Y;F) \geq I(Y;g(F)) = I(Y;\hat{Y}) = -\frac{1}{2}\log[1-\rho^2(Y,\hat{Y})] = -\frac{1}{2}\log[1-R^2].$$

Machine learning evaluation functions and mutual information have been equated many times in the feature importance literature. Covert et al. (2020) demonstrated equivalence when the Bayes classifier is known and cross entropy loss is used. In a simple example, Catav et al. (2020) used mutual information directly as the evaluation function. The connection between machine learning evaluation functions and mutual information was further used by Sutera et al. (2021) to relate random forest feature importance with Shapely values.

B Additional information about marginal contribution feature importance (MCI)

Two of the methods that are compared with MCI in Catav et al. (2021) include ablation and bivariate association. Ablation methods determine feature importance based on the difference in accuracy between the full model and the full model without the feature of interest, i.e. $A_\nu(x_i) = \nu(F) - \nu(F \setminus \{x_i\})$. Bivariate methods are among the most popular methods for genome-wide association studies (Consortium et al., 2007; Easton et al., 2007; Sun et al., 2021). In this method, the feature importance is given by the difference in the evaluation function of the model with just the feature of interest and the null model, i.e. $B_\nu(x_i) = \nu(x_i) - \nu(\emptyset)$. The three feature importance axioms proposed by Catav et al. (2021) were partially motivated by the shortcomings of these two methods.

1. **Marginal contribution**: Ablation methods may underestimate the importance of features when the correlation between features is high. In these scenarios, $\nu(F)$ may be approximately equal to $\nu(F \setminus \{x_i\})$ even in cases where x_i is highly related to the response. Because of this, the importance of a feature $I_\nu(x_i)$ should be at least as large as the importance given by ablation methods: $I_\nu(x_i) \geq A_\nu(x_i) = \nu(F) - \nu(F \setminus \{x_i\})\ \forall x_i \in F$.
2. **Elimination**: Bivariate methods may underestimate the importance of features in cases where interactions exist between features. Many high-order interactions may be present in the data, so eliminating features from the feature set could prevent the detection of an important interaction. Thus, eliminating features from F should only be able to decrease the feature importance of x_i.
3. **Minimalism**: Catav et al. (2021) decided to impose the minimalism axiom so that MCI can be unique. If $I_\nu(x_i)$ satisfies the first two axioms, then multiplying $I_\nu(x_i)$ by any constant $\lambda > 1$ would not change this. The minimalism axiom helps disambiguate MCI from these trivial variations.

We intentionally excluded some of the MCI axioms and properties included by Catav et al. (2021) when proposing axioms for explaining data in Section 2. Most importantly, the marginal contribution axiom is not included because it conflicts directly with the blood relation axiom. Indeed, ablation methods could give too much importance from a scientific inference perspective. For example, in the collider example presented by Harel et al. (2022), they present the causal graph $Y \leftarrow S \rightarrow G \leftarrow E$, where S is unmeasured. Let $F = \{E, G\}$ be used to predict Y. Then, the marginal contribution axiom requires that feature E is given importance. Indeed, if we know G, then feature E can help predict the response by denoising G to recover information from the unobserved cause S. Thus, $I_\nu(E) \geq A_\nu(E) = \nu(\{E,G\}) - \nu(\{G\}) > 0$. However, as stated in Harel et al. (2022), feature E has no relation to the response Y, since it can be thought of as a noise variable, so it would be more reasonable to give E zero importance. We note that E is given zero importance under the blood relation axiom, so the blood relation axiom is more reasonable and justified compared to the marginal contribution axiom. In contrast, G inherently contains information about Y via S, but this information is noised up by E. Therefore, although E can be used to denoise G and predict Y better, only G should be given importance when explaining the data when $F = \{E, G\}$, and indeed, G is blood related to Y. We note that UMFI obeys the blood relation axiom under some assumptions, and hence does not obey the marginal contribution axiom. We additionally exclude the minimalism axiom since we do not prioritize uniqueness.

C Additional information about ultra-marginal feature importance (UMFI)

Theorem C.1 (Existence of optimal preprocessing $\hat{S}^F_{x_i}$ when all features are jointly Gaussian)**.** *Let $x_i \in F$ and suppose that all random variables in the random vector F are joint normally distributed, then there exists a preprocessing $S^F_{x_i}$ that is optimal.*

Proof. A preprocessing $S^F_{x_i}$ can be obtained via multiple linear regression (after mean centering) with the model:

$$F \setminus \{x_i\} = \beta x_i + \epsilon,$$

where $\epsilon = S^F_{x_i}$, x_i is a feature in F, and β is the column vector of size $p-1$ containing regression coefficients $\beta_1, \beta_2, ..., \beta_{p-1}$ that minimize the sum of squared errors between x_i and a linear function of each other variable in $F \setminus \{x_i\}$.

To show that $S^F_{x_i}$ is an optimal preprocessing (Definition 1), it suffices to show that $S^F_{x_i} \perp\!\!\!\perp X_i$ and that $I(Y;F) = I(Y; S^F_{x_i}, X_i)$, since $S^F_{x_i}$ is a function of F by construction.

From the normal equations and the definition of covariance, we know that $Cov(S^F_{x_i}, X_i) = 0$, as shown in the proof of Theorem E.3. Since $S^F_{x_i} = F \setminus \{x_i\} - \beta x_i$, and all features in F are joint normally distributed, it follows that $(S^F_{x_i}, x_i)$ is joint normally distributed as well, since $(S^F_{x_i}, x_i)$ can be obtained via the linear transformation $AF = (S^F_{x_i}, x_i)$, where the main diagonal entries of A are 1, the other $|F|-1$ entries of the column corresponding to x_i are given by the entries of $-\beta$, and all other entries are 0. Without loss of generality, we may reorder the columns of the matrix such that the last column is attributed to feature x_i, and write

$$A = \begin{bmatrix} 1 & 0 & \dots & \dots & -\beta_1 \\ 0 & 1 & 0 & \dots & -\beta_2 \\ \vdots & & \ddots & & \\ 0 & 0 & \dots & \dots & 1 \end{bmatrix} \qquad A^{-1} = \begin{bmatrix} 1 & 0 & \dots & \dots & \beta_1 \\ 0 & 1 & 0 & \dots & \beta_2 \\ \vdots & & \ddots & & \\ 0 & 0 & \dots & \dots & 1 \end{bmatrix}.$$

Hence, $Cov(X_i, S^F_{x_i}) = 0 \implies S^F_{x_i} \perp\!\!\!\perp X_i$ from the properties of multivariate Gaussians.

To prove the second claim $I(Y;F) = I(Y; S^F_{x_i}, X_i)$, by Theorem A.5, it suffices to show that the map $h(F) = (S^F_{x_i}, x_i) = AF$ is injective. This is immediate from the fact that the matrix A, defined above, is invertible and thus bijective.

□

Theorem C.2 (Elimination axiom assuming optimal transport with chaining)**.** *Let $x_i \in F$, $x_{p+1} \notin F$, and $\nu(S)$ is positively linearly related to $I(Y;S)$. When preprocessing is performed using optimal transport with chaining, $U_\nu^{F,Y}(x_i) \leq U_\nu^{F\cup\{x_{p+1}\},Y}(x_i)$.*

Proof. Let $S^{F\cup\{x_{p+1}\}}_{x_i}$ be the preprocessed version of $F \cup \{x_{p+1}\}$ relative to x_i and let $S^F_{x_i}$ be the preprocessed version of F relative to x_i. By optimal transport with chaining (Johndrow and Lum, 2019), we may assume that $S^{F\cup\{x_{p+1}\}}_{x_i}$ obeys the form $S^{F\cup\{x_{p+1}\}}_{x_i} = S^F_{x_i} \cup \tilde{x}$ and that $S^F_{x_i}, X_i, \tilde{X}$ are mutually independent. It follows from the supermodularity of mutual information under independence (Theorem A.3) that

$$\begin{aligned} U_\nu^{F\cup\{x_{p+1}\},Y}(x_i) &= aI(Y; S^{F\cup\{x_{p+1}\}}_{x_i}, X_i) + c - (aI(Y; S^{F\cup\{x_{p+1}\}}_{x_i}) + c) \\ &= aI(Y; S^F_{x_i}, \tilde{X}, X_i) + c - (aI(Y; S^F_{x_i}, \tilde{X}) + c) \\ &\geq aI(Y; S^F_{x_i}, X_i) + c - (aI(Y; S^F_{x_i}) + c) = U_\nu^{F,Y}(x_i). \end{aligned}$$

□

Lemma C.3 (Equivalence of optimal preprocessing equivalence classes under redundant information and duplicate features of interest)**.** *If $\hat{x} \in \mathcal{I}(F)$, then $[\hat{S}^F_{x_i}] \equiv [\hat{S}^{F\cup\{\hat{x}\}}_{x_i}]$. If $\hat{x} = h(x_j)$ and h is bijective, then $[\hat{S}^{F\cup\{\hat{x}\}}_{x_j}] \equiv [\hat{S}^{F\cup\{\hat{x}\}}_{\hat{x}}]$.*

Proof. Recall that an optimal preprocessing given a feature set F and a feature of interest x_i is defined in Definition 1. To prove $[\hat{S}^F_{x_i}] \equiv [\hat{S}^{F\cup\{\hat{x}\}}_{x_i}]$, we prove that for any $x_i \in F$ all optimal preprocessings $\hat{S}^F_{x_i}$ are also optimal preprocessings in $[\hat{S}^{F\cup\{\hat{x}\}}_{x_i}]$, and that all optimal preprocessings $\hat{S}^{F\cup\{\hat{x}\}}_{x_i}$ are also optimal preprocessings in $[\hat{S}^F_{x_i}]$.

We first note that properties 1 and 2 in Definition 1 are equivalent for $\hat{S}^F_{x_i}$ and $\hat{S}^{F\cup\{\hat{x}\}}_{x_i}$. For property 1, a function with repeated arguments can be defined to be equal to the same function without repeated arguments. For property 2, the feature of interest x_i is consistent across both optimal preprocessings, so both preprocessings are independent of X_i. Lastly, since

mutual information is invariant under duplicate information and since $\hat{S}_{x_i}^F$ and $\hat{S}_{x_i}^{F\cup\{\hat{x}\}}$ each satisfy their respective 3rd property,

$$I(Y;F,\hat{X}) = I(Y;\hat{S}_{x_i}^{F\cup\{\hat{x}\}},X_i) = I(Y;F) = I(Y;\hat{S}_{x_i}^F,X_i). \tag{7}$$

Hence, the final property is also equivalent across both equivalence classes of optimal preprocessings, and we conclude $[\hat{S}_{x_i}^F] \equiv [\hat{S}_{x_i}^{F\cup\{\hat{x}\}}]$.

Similarly, to prove that $[\hat{S}_{x_j}^{F\cup\{\hat{x}\}}] \equiv [\hat{S}_{\hat{x}}^{F\cup\{\hat{x}\}}]$ if $\hat{x} = h(x_j)$ for some bijective function h, we note that the first property is equivalent for both optimal preprocessings, since they take place over the same feature set $F \cup \{\hat{x}\}$. Then, we note that $\hat{S}_{x_j}^{F\cup\{\hat{x}\}} \perp\!\!\!\perp X_j \implies \hat{S}_{x_j}^{F\cup\{\hat{x}\}} \perp\!\!\!\perp h(X_j) = \hat{X}$, and similarly, $\hat{S}_{\hat{x}}^{F\cup\{\hat{x}\}} \perp\!\!\!\perp \hat{X} \implies \hat{S}_{\hat{x}}^{F\cup\{\hat{x}\}} \perp\!\!\!\perp h^{-1}(\hat{X}) = X_j$. Finally, since mutual information is invariant under homeomorphic reparametrization of marginal variables Kraskov et al. (2004),

$$\begin{aligned}
I(Y;F) &= I(Y;\hat{S}_{\hat{x}}^{F\cup\{\hat{x}\}},\hat{X}) = I(Y;\hat{S}_{\hat{x}}^{F\cup\{\hat{x}\}},h^{-1}(\hat{X})) = I(Y;\hat{S}_{\hat{x}}^{F\cup\{\hat{x}\}},X_j)\\
I(Y;F) &= I(Y;\hat{S}_{x_j}^{F\cup\{\hat{x}\}},X_j) = I(Y;\hat{S}_{x_j}^{F\cup\{\hat{x}\}},h(X_j)) = I(Y;\hat{S}_{x_j}^{F\cup\{\hat{x}\}},\hat{X})
\end{aligned}$$

Since all 3 properties are equivalent for both optimal preprocessings, we conclude that $[\hat{S}_{x_i}^F] \equiv [\hat{S}_{x_i}^{F\cup\{\hat{x}\}}]$. □

We note that preprocessings $S_{x_i}^F$ and $S_{x_i}^{F\cup\{\hat{x}\}}$ may be interchangeable without being optimal, and that the interchangeability of these preprocessings is a sufficient condition for UMFI satisfying the redundant information invariance axiom, as long as $\nu(\cdot) = I(Y;\cdot)$. For example, interchangeability of preprocessings also holds when the removal of dependencies on a feature x_i is done in a pairwise fashion (see Algorithm 3), as well as when preprocessings is performed via optimal transport with chaining (Johndrow and Lum, 2019).

Theorem C.4 (Blood relation axiom assuming faithfulness)**.** *Let $x_i \in F$, $\nu(S)$ is positively linearly related to $I(Y;S)$, and suppose that the data is generated from a structural causal model C with corresponding directed causal graph G so that the entailed distribution is faithful to G. Assume also that there exists an structural causal model with graph G' that contains the variables X_i, $S_{x_i}^F$, and Y, where the distribution of all its variables is faithful to the graph G'. If the preprocessing $S_{x_i}^F \perp\!\!\!\perp X_i$, then $U_\nu^{F,Y}(x_i) > 0$ if and only if $X_i \in BR_G(Y)$.*

Proof. As shown in the proof of Theorem 3.1 in the main text, we may apply the definition of UMFI and ν, the assumption $S_{x_i}^F \perp\!\!\!\perp x_i$, and properties of mutual information and conditional independence to obtain

$$U_\nu^{F,Y}(x_i) = 0 \iff aI(Y;X_i|S_{x_i}^F) + c - c = 0 \iff X_i \perp\!\!\!\perp Y|S_{x_i}^F \iff X_i \perp\!\!\!\perp (Y,S_{x_i}^F) \implies X_i \perp\!\!\!\perp Y$$

We note that the last implication comes from the contraction axiom (Dawid, 1979), and it can be strengthened to an equivalence as long as we can prove $X_i \perp\!\!\!\perp (Y,S_{x_i}^F)$ using the assumptions $X_i \perp\!\!\!\perp Y$ and $X_i \perp\!\!\!\perp S_{x_i}^F$. Since X_i, Y, and $S_{x_i}^F$ belong to an SCM with graph G', and the entailed distribution of this SCM is faithful to G', then $X_i \perp\!\!\!\perp Y$ and $X_i \perp\!\!\!\perp S_{x_i}^F$ imply that X_i is d-separated from both Y and $S_{x_i}^F$ by $\emptyset$. Therefore, $X_i \perp\!\!\!\perp (Y,S_{x_i}^F)$, and $U_\nu^{F,Y}(x_i) = 0 \iff X_i \perp\!\!\!\perp Y$.

Also, if the data is faithful to the causal graph G, then $X_i \perp\!\!\!\perp Y$ is equivalent to $X_i \notin BR_G(Y)$, which would conclude the proof of the blood relation axiom. We explicitly provide the details.

If $X_i \notin BR_G(Y)$, then $X_i \perp\!\!\!\perp Y$ follows from the global Markov property and the fact that X_i and Y are d-separated by the empty set. Indeed, every path from X_i to Y must have at least one collider. We consider two cases. (1) The edge coming out of Y is outgoing. Then since X_i is not a descendent of Y, the path must reverse its orientation at some vertex before meeting X_i. That vertex is a collider. (2) The edge connecting to Y points towards Y. Then the path must reverse its orientation at some point since X_i is not an ancestor of Y. The path must then reverse another time because otherwise, X_i would share a common ancestor with Y (the vertex of the first reversal). The vertex with the second reversal is a collider.

Conversely, let $X_i \in BR_G(Y)$. By the faithfulness assumption, it suffices to show that X_i and Y are d-connected by the empty set. Since $X_i \in BR_G(Y)$, there are two possible cases: either there is a directed path between X_i and Y, or X_i and Y share a common ancestor. In the first case, we simply choose the directed path between X_i and Y and observe that there cannot be a collider. Similarly, in the second case, we may pick the path beginning at Y and trace it up to the common ancestor and then travel to X_i. There can be no colliders along the path since every vertex has at least one outgoing edge by construction. Also, the empty set cannot contain any non-colliders.

□

Theorem C.5 (Blood relation axiom in the absence of interactions)**.** *Suppose that there is no synergistic information $I_{syn}(Y; S^F_{x_i}, X_i)$ about Y between X_i and $S^F_{x_i}$ for all $x_i \in F$, and that $S^F_{x_i} \perp\!\!\!\perp X_i$. Then, if the graphical model obeys the global Markov property and faithfulness and $\nu(S)$ is positively linearly related to $I(Y; S)$, then $U^{F,Y}_\nu > 0$ if and only if $X_i \in BR_G(Y)$.*

Proof. As in the proof of Theorem C.4, it suffices to show that $I(Y; X_i|S^F_{x_i}) = 0$ if and only if $X_i \notin BR_G(Y)$. We may rewrite $I(Y; X_i|S^F_{x_i}) = 0$ as $I(Y; S^F_{x_i}, X_i) = I(Y; S^F_{x_i})$.

Though it is fairly controversial (Williams and Beer, 2010; Griffith and Koch, 2014), some definitions of partial information decomposition imply that independent predictors cannot contain redundant information between them (Kolchinsky, 2022; Harder et al., 2013). Using partial information decomposition (Williams and Beer, 2010), and since $S^F_{x_i} \perp\!\!\!\perp X_i \implies I_{red}(Y; S^F_{x_i}, X_i) = 0$, we may decompose $I(Y; S^F_{x_i}, X_i)$ as

$$I_{unq}(Y; X_i) + I_{unq}(Y; S^F_{x_i}) + I_{syn}(Y; S^F_{x_i}, X_i).$$

where we note that, because of the lack of redundancy, $I(Y; X_i) = I_{uniq}(Y; X_i)$ and that $I(Y; S^F_{x_i})$ captures the unique information that $S^F_{x_i}$ shares with Y as well as synergistic information within the random vector $S^F_{x_i}$ that is shared with Y. As proven in Theorem C.4, $I(Y; X_i) = 0$ if $X_i \notin BR_G(Y)$ and $I(Y; X_i) > 0$ if $X_i \in BR_G(Y)$ by the global Markov property and faithfulness. Since $I_{syn}(Y; S^F_{x_i}, X_i) = 0$ by assumption, this gives us the desired statement $I(Y; S^F_{x_i}, X_i) = I(Y; S^F_{x_i})$ if and only if $X_i \notin BR_G(Y)$. □

D Additional information about other feature importance methods

Historically, feature importance methods were developed in the pursuit of scientific questions, but current research in this area typically focuses on model explainability or model optimization. Early forms of feature importance assessed the strength of the relationships between variables within animal biology or human psychology using methods such as the correlation coefficient (Galton, 1889), Spearman's rank correlation coefficient (Spearman, 1961), multiple linear regression (Darlington, 1968), and partial correlation (Wright, 1921). Although these methods are perfectly interpretable, they are inadequate for modelling and therefore explaining complex data, since they cannot quantify the unknown interactions between multiple features. To counteract this severe limitation, Breiman was instrumental with his introduction of variable importance within classification and regression trees (Breiman et al., 2017). At that time, Breiman seemed more concerned about the true strength of the relationships between the explanatory variables and the response, as he posited that a feature that is related to the response should be given some importance even if it does not appear in the final model (Breiman et al., 2017). However, starting with Breiman's random forests, feature importance began to prioritize machine learning model explanation rather than data exploration. A good overview of the properties of some popular feature importance metrics is shown in Covert et al. (2020).

E Preprocessing methods for removing dependencies

Finding information preserving independent representations of our data is the central step of UMFI. These representations were first considered for AI fairness and privacy algorithms in order to give unbiased predictions in the face of sensitive attributes. For example, if one wants to remove the influence of race on recidivism likelihood predictions, preprocessing methods can be used to alter the original dataset such that the set of predictors are independent of race. In the following subsections, we discuss how optimal transport and linear regression can be used for finding these representations.

E.1 Optimal transport

Most of the results and methods explained in this section can be found in Johndrow and Lum (2019). In this section, we denote features in the feature set F by X_j or X_i to emphasize that they are random variables, rather than the previously used x_j and x_i, where the former is used to denote observations x_j sampled from X_j instead. To obtain a preprocessing $S^F_{X_i}$, we may remove the dependencies of x_i from each $X_j \in F \setminus \{X_i\}$ with minimal information loss with respect to X_j. To do so using optimal transport, we consider the Monge problem:

$$g_c(X_j, \tilde{X}_j) = \inf_{g: g(X_j) \sim \tilde{X}_j} \mathbb{E}[c(X_j, g(X_j))] = \inf_{g: g(X_j) \sim \tilde{X}_j} \int_{\mathbb{R}} c(x_j, g(x_j)) d\mu(x_j). \tag{2.1.1}$$

The quantity $g_c(X_j, \tilde{X}_j)$ represents the transportation cost of moving X_j to $\tilde{X}_j$ with respect to some cost function c, and in our case, we desire $\tilde{X}_j \perp\!\!\!\perp X_i$. It is natural to use $c(x_j, \tilde{x}_j) = d^q(x_j, \tilde{x}_j)$, where d is the Euclidean norm. The transportation cost is also given by the Wasserstein-q distance, $g_c(X_j, \tilde{X}_j) = \mathcal{W}_q^q(X_j, \tilde{X}_j)$, defined below for one-dimensional distributions.

$$\mathcal{W}_q(X_j, \tilde{X}_j)^q = \int_0^1 |F^{\leftarrow}(p) - \tilde{F}^{\leftarrow}(p)|^q dp,$$

where F_j and $\tilde{F}_j$ are the CDFs of X_j and $\tilde{X}_j$, and $F_j^{\leftarrow}(p) = \sup_{x_j \in \mathbb{R}} F_j(x_j) \leq p$. It can be shown that given any continuous one dimensional distributions X_j and $\tilde{X}_j$, the optimal transport map $g : X_j \to \tilde{X}_j$ is given by $g = \tilde{F}_j^{\leftarrow} \circ F_j$.

Theorem E.1. *Let X be a r.v. with density f and CDF F. Let $\tilde{X}$ have CDF $\tilde{F}$. Then $g = \tilde{F}^{\leftarrow} \circ F$ is the minimizer to* (2.1.1)*. Hence, g optimally transports X to $\tilde{X} = \tilde{F}^{\leftarrow}(F(X))$.*

Proof. We show $\mathbb{E}[|X - g(X)|^q] = \int_0^1 |F^{\leftarrow}(p) - \tilde{F}^{\leftarrow}(p)|^q dp$ for $g = \tilde{F}^{\leftarrow} \circ F$

$$\begin{aligned}\mathbb{E}[|X - g(X)|^q] &= \int_{-\infty}^{\infty} |x - \tilde{F}^{\leftarrow}(F(x))|^q f(x) dx \\ &= \int_{-\infty}^{\infty} |F^{\leftarrow}(F(x)) - \tilde{F}^{\leftarrow}(F(x))|^q f(x) dx = \int_0^1 |F^{\leftarrow}(p) - \tilde{F}^{\leftarrow}(p)|^q dp\end{aligned}$$

□

Theorem E.2. *Let $F_{j|x_i}(x) = P(X_j \leq x_j | X_i = x_i)$ denote the CDF of $X_j|\{X_i = x_i\}$. Then $g = \tilde{F}^{\leftarrow} \circ F_{j|x_i}$ optimally transports $X_j|\{X_i = x_i\}$ to $\tilde{X}_j \perp\!\!\!\perp X_i$ for any CDF $\tilde{F}$*

Proof. We apply Theorem E.1 on the random variable $X_j|\{X_i = x_i\}$ and note that $X_j|\{X_i = x_i\}$ is independent of X_i. In particular, $g(X_j|X_i = x_i) \perp\!\!\!\perp X_i$ for any choice of $\tilde{F}$. □

Theorem E.2 suggests an algorithm for transporting data $(x_{j1}, ..., x_{jn})$ sampled from X_j, to $(\tilde{x}_{j1}, ..., \tilde{x}_{jn}) \perp\!\!\!\perp (x_{i1}, ..., x_{in})$. Since x_{jk} is taken jointly with x_{ik}, as they are attributes coming from the kth sample in the dataset, then x_{jk} is a realization of the distribution $X_j|\{X_i = x_{ik}\}$. Consequently, for each $k = 1, ..., n$, we should transport x_{jk} to $\tilde{x}_{jk} = \tilde{F}^{\leftarrow}(F_{j|x_{ik}}(x_{jk}))$, where we may pick any CDF $\tilde{F}$. This procedure can also adapted for features sampled from discrete r.v's, as shown in Johndrow and Lum (2019).

Algorithm 2: Algorithm for removing dependencies of X_i from X_j

Require: $X_j = [x_{j1}, ..., x_{jn}], X_i = [x_{i1}, ..., x_{in}]$, $X_j|(X_i = x_{ik}) \sim F_{j|x_{ik}}$, $\tilde{F}$ is a CDF
  for $k = 1, ..., n$ **do**
    $\tilde{x}_{jk} = \tilde{F}^{\leftarrow}(F_{j|x_{ik}}(x_{jk}))$
  end for
  return $\tilde{X}_j = [\tilde{x}_{j1}, ..., \tilde{x}_{jn}]$

We denote the result of the algorithm by $\tilde{X}_j = \tilde{F}^{\leftarrow}(F_{j|X_i}(X_j))$ and would ideally pick $\tilde{F}$ such that it minimizes the transportation cost $g_c(X_j, \tilde{X}_j) = g_c(X_j, \tilde{F}^{\leftarrow}(F_{j|X_i}(X_j)))$ across all CDFs $\tilde{F}$ in order to minimize information loss. However, in practice, the choice of $\tilde{F}$ does not matter much. In fact, as long as the support of $\tilde{F}$ is at least a large as the support of F_j, the cdf of X_j, then any rank-based prediction rule, e.g. random forest, will be invariant to the choice of $\tilde{F}_j$ (Johndrow and Lum, 2019). A standard choice for $\tilde{F}_j$ is F_j so that we can recover the original quantiles of X_j.

Furthermore, $F_{j|x_{ik}}$ is not usually known and must be estimated from the data. For example, this can be done by splitting X_i into N quantiles and using the empirical CDF $P(X_j \leq x_j | X_i \in x_{ik}$'s quantile$)$. The ability of this method to remove dependencies on X_i from X_j relies significantly on the accuracy of this estimate.

We may iterate Algorithm 2 over each feature in $F \setminus \{X_i\}$ to obtain pairwise independence between the transported variables $\tilde{X}_j$ and X_i. It is also possible to iterate Algorithm 2 via chaining to achieve mutual independence between the transformed variables $\tilde{X}_j$ and X_i (Johndrow and Lum, 2019, Section 3.2). However, this is computationally expensive,

Algorithm 3: Algorithm for estimating $S^F_{X_i}$ via pairwise optimal transport

Require: $X_i = [x_{i1}, ..., x_{in}]$, $X_j = [x_{j1}, ..., x_{jn}]$ for X_j in $F \setminus X_i$
  $S^F_{X_i} = \emptyset$
  for X_j in $F \setminus \{X_i\}$ **do**
    $\tilde{X}_j$ = output of Algorithm 2 with X_j and X_i
    add $\tilde{X}_j$ to S^F_Z
  end for
  return $S^F_{X_i}$

and pairwise independence should suffice for an accurate UMFI score, as will be explored further in Section F. Step 2 of Algorithm 1 in the main paper can therefore be implemented with Algorithm 3.

In other words, we may estimate $S^F_{X_i}$ as:

$$S^F_{X_i} = \{F_j^{\leftarrow}(F_{j|X_i}(X_j)) : X_j \in F \setminus \{X_i\}\}.$$

E.2 Linear regression

The most basic method for removing dependencies is linear regression. Even though it is quite simple, it can be shown to be optimal with a few assumptions (Theorem C.1). This preprocessing technique is implemented in the popular Python package *fairlearn* (Bird et al., 2020; Matthijs et al., 2019).

To reiterate, removing dependencies requires methods to make a feature or set of features S independent of a protected attribute x_i, while keeping as much of the original information as possible. The overarching idea of linear regression as a preprocessing technique is that under the assumption that the residuals and the protected attribute are jointly Gaussian, the residuals can be utilized as a representation of S, which is independent of x_i.

Theorem E.3. *The residuals ϵ of a simple linear regression model have zero covariance with the predictor X.*

Proof. (1) From the normal equations, the definition of covariance, and the fact that $\mathbb{E}[\epsilon] = 0$, it follows that

$$\begin{aligned} &Cov(X, \epsilon) = \mathbb{E}[X^T\epsilon] - \mathbb{E}[\epsilon]\mathbb{E}[X] = \mathbb{E}[X^T\epsilon] = \mathbb{E}[X^T(Y - X\beta)] \\ &= \mathbb{E}[X^T(Y - X(X^TX)^{-1}X^TY))] = \mathbb{E}[X^TY - X^TX(X^TX)^{-1}X^TY] = \mathbb{E}[X^TY - X^TY] = 0 \end{aligned}$$

□

Thus, in step 2 of the algorithm for UMFI (Algorithm 1), we can estimate

$$S^F_{X_i} = \{\epsilon_j = X_j - \beta_{0,j} - \beta_{1,j}X_i : X_j \in F \setminus \{X_i\}\}$$

where $\beta_{0,j}$ is the intercept term and $\beta_{1,j}$ is the slope term of the linear regression model $X_j = \beta_{0,j} + \beta_{1,j}X_i + \epsilon_j$.

F Experiments comparing linear regression and optimal transport

In the following subsections, we compare the ability of linear regression and pairwise optimal transport to remove the information of a feature from data while distorting the original data as little as possible. It can be concluded that while linear regression works optimally when the data is jointly Gaussian, on real data, such as the BRCA dataset, pairwise optimal transport can find independent representations of the data, while linear regression fails (Section F.1).

To implement UMFI paired with linear regression, we only remove dependencies when the regression slope coefficient is statistically significant (p-value < 0.01). To implement UMFI paired with pairwise optimal transport, when removing dependencies on the feature x_i from the dataset, we estimate $F_{j|x_{ik}}$ by breaking up x_i into quantiles of size 150 and running linear regression on each quantile. The new independent predictors are then given by the values of the inverse empirical CDF of the residuals from the mentioned linear regression models.

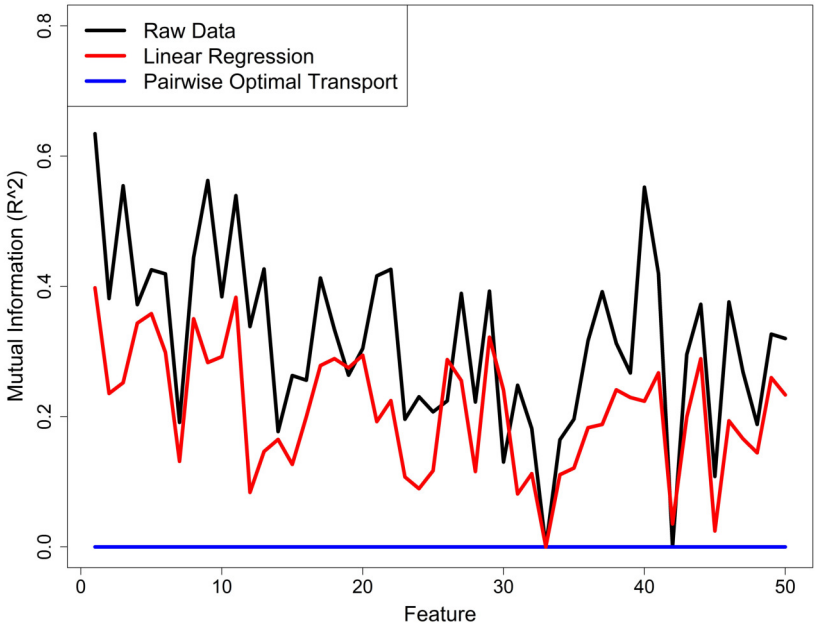

Figure 6: The coefficient of determination (random forest OOB-R^2) between the ith feature in the BRCA dataset and all other features is plotted (black) for each $i \in \{1, 2, ...50\}$. The R^2 value between the ith feature and all other features after preprocessing with linear regression (red) and optimal transport (blue) is also plotted.

F.1 Removing dependencies

It is crucial for our linear regression and optimal transport preprocessing methods to remove the information associated with the feature of interest, x_i, from the rest of the dataset $F \setminus \{x_i\}$. Therefore, we would like the preprocessed dataset $S^F_{x_i}$ to share zero mutual information with x_i. The mutual information $I(X_i; S^F_{x_i})$ is difficult to calculate, but it is closely related to the optimal predictor of x_i given $S^F_{x_i}$ (Song et al., 2019). For example, if $I(X_i; S^F_{x_i}) = 0$, as is desired, then the optimal predictor of x_i will have zero accuracy when given $S^F_{x_i}$ as input. If the opposite is true and $S^F_{x_i}$ contains all of the information from x_i, then an optimal predictor of x_i should be able to perfectly predict x_i from the given information in $S^F_{x_i}$. In the following experiments, we assume that random forests can form the optimal predictor of x_i given $S^F_{x_i}$. We use the OOB-R^2 coming from the random forest model as a approximate measure of the mutual information between x_i and the transformed dataset $S^F_{x_i}$.

We used the BRCA dataset with 50 features to test the ability of optimal transport and linear regression to remove dependencies (Covert et al., 2020; Catav et al., 2020). All 50 features are continuous and the response is categorical. For each individual feature, we first use random forest OOB-R^2 to give a approximate measure of the mutual information $I(X_i; F \setminus \{x_i\})$ between the feature of interest x_i and the other 49 features. We then consider the case where the 49 remaining features are preprocessed to have dependencies on x_i removed via linear regression or pairwise optimal transport. Similarly, random forest's OOB-R^2 is used to give a approximate measure of $I(X_i; S^F_{x_i})$.

The results are plotted in Figure 6. It is clear that the raw data (black line) shares considerable information across features. Most features can be predicted from the other untransformed features with an accuracy of $R^2 > 0.2$ and many can even be predicted with accuracies over 0.4. Since the data has extremely nonlinear dependencies between features, simple linear regression is unable to remove all the mutual information between the protected attributes and the rest of the features. Indeed, the data certainly cannot be approximated with multivariate Gaussians. Conversely, pairwise optimal transport can successfully remove most of the mutual information present in the data. For all 50 features in the dataset, x_i cannot be predicted successfully by random forest (OOB-$R^2 = 0$) from the other features after $F \setminus x_i$ is transformed with pairwise optimal transport.

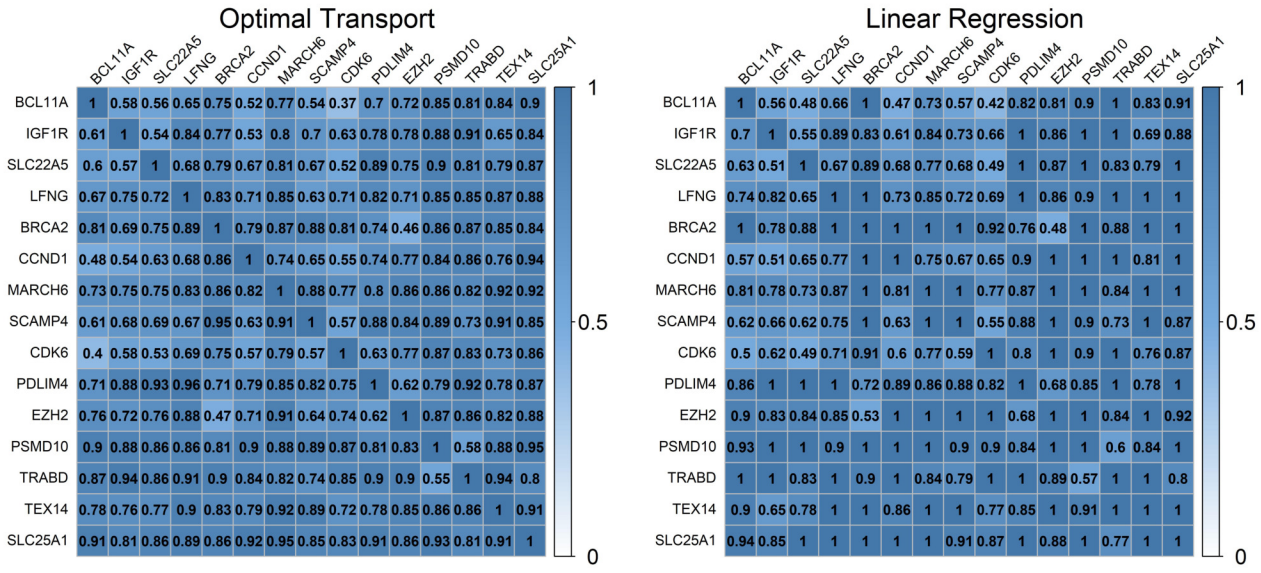

Figure 7: Cell (i, j) indicates how similar the j^{th} variable in the BRCA dataset is compared to its transformation via pairwise optimal transport or linear regression with respect to feature i. This is measured with the maximal information coefficient, which is comparable to R^2. To make the plots more clear and accessible, only the first 15 features are shown.

F.2 Distortion

Not only do we require that the transformed features are independent of the feature of interest, but we also require that as much of the information present in the original data is preserved in the transformed data. To measure the amount of distortion imposed on the original data, we measure the dependence between the original and perturbed data using the maximal information coefficient (Kinney and Atwal, 2014). For each feature in the BRCA dataset with 50 features (Covert et al., 2020; Catav et al., 2020), the information from the current feature is removed from all other features with either linear regression or pairwise optimal transport (Figure 7).

Linear regression does not distort the transformed features in most cases. The dependence between the original and perturbed features usually remains near 1, though the dependence does go as low as 0.42 in one case (Figure 7). While linear regression transformed these features with minimal distortion, these results are moot since linear regression failed to remove the original dependencies in a significant way, which was the main goal of the method (Figure 6).

Compared to linear regression, pairwise optimal transport has a much more sizable effect on the distorted features, though this may have been necessary to completely remove dependence. The dependence between original and perturbed features mostly ranges from 0.6-0.9, though some are as low as 0.37 (Figure 7). While only the first 15 features are shown, the results are similar for the other 35 features.

G Further feature importance experiments

This section is comprised of additional experiments performed on the simulated data introduced in Section 4.1, the BRCA dataset with permuted random genes, the original BRCA dataset with unpermuted random genes (Tomczak et al., 2015; Covert et al., 2020; Catav et al., 2021), and the CAMELS hydrology dataset (Addor et al., 2017). MCI and UMFI used either random forests or extremely randomized trees (Breiman, 2001; Geurts et al., 2006). Both of these, as well as ablation and permutation importance were implemented using the *ranger* R package (Wright and Ziegler, 2015), while conditional permutation importance was implemented with the *randomForest* and *permimp* packages (Debeer et al., 2021; Liaw et al., 2002). All experiments were run in Microsoft R Open Version 4.0.2.

G.1 Extra experiments on simulated data

We repeat our previous experiments on simulated data from Section 4.1 to test how ablation, permutation importance (PI), and conditional permutation importance (CPI) behave in the presence of nonlinear interactions (Section G.1.1), correlated interactions (Section G.1.2), correlation (Section G.1.3), and blood and non-blood related features (Section G.1.4). Further, we test how using extremely randomized trees instead of random forests for MCI and UMFI changes the results of the same simulation experiments. Although other methods such as XGBoost (Chen et al., 2015) could have been implemented for these experiments, XGBoost requires greater care when optimizing hyperparameters, so we chose to use extremely randomized trees instead, which is faster than random forests and provides similarly good predictions (Geurts et al., 2006). Both random forests and extremely randomized trees are not very sensitive to hyperparameter selection (Probst et al., 2019). For these simulation studies, we also perturb the size of the quantiles used by UMFI_OT. We now use quantiles of size 30 instead of size 150. Quantiles of size 30 worked better on the hydrology data used in later experiments, so we test to see if the simulation results are sensitive to this choice in quantile size for dependency removal via optimal transport.

G.1.1 Nonlinear interactions

The first experiment on simulated data handles the case where two variables, x_1 and x_2, interact in a nonlinear way in the response Y. As explained in Section 4.1.1, we should expect x_1 and x_2 to contribute more than half of the total importance, while x_3 and x_4 should be important, but less important compared to x_1 and x_2. Figure 8a shows that ablation, PI, and CPI all provide accurate scores.

When tested with extremely randomized trees, the nonlinear interactions simulation experiment results for MCI and UMFI, shown in Figure 8e, remain mostly unchanged compared to the results from the experiment with random forests given in Figure 1a.

G.1.2 Correlated interactions

The second experiment considers the case where two correlated variables, x_1 and x_2, interact together in the response Y. Thus, as explained in Section 4.1.2, we should expect x_1 and x_2 to have more importance compared to x_3 and x_4. Figure 8b shows that ablation, PI, and CPI all correctly weigh the importance of x_1 and x_2 as high relative to x_3 and x_4. The only notable difference is that the ablation method attributes an additional $\sim 3\%$ importance to each of x_1 and x_2 compared to PI, CPI, MCI, and UMFI (Figure 8b).

When tested with extremely randomized trees instead of random forests, the correlated interaction simulation experiment results (Figure 8f) for MCI and UMFI are similar to the earlier results shown in Figure 1b. MCI gave slightly more importance to x_1 and x_2 compared to x_3 and x_4, though the differences are seemingly insignificant. On the other hand, both UMFI methods gave significantly more importance to x_1 and x_2 compared to x_3 and x_4, as expected.

G.1.3 Correlation

The third experiment tests how the metrics allocate importance to correlated features. As explained in Section 4.1.3, x_1 and x_2 should remain around the same relative importance, and $x_3 = x_1 + \epsilon$, should have just slightly less importance compared to x_1 and x_2. Figure 8c indicates that CPI and ablation give near zero importance to the two heavily correlated features x_1 and x_3. This aligns with the discussion in Section A.2 about methods motivated by feature selection since these methods base their scores on the importance of a feature conditioned on all other variables present in the model. Ablation performs similarly to CPI in this test, albeit with slightly less drastic results. Finally, we see that PI splits the importance detected from x_1 and x_3 proportionally across both features. This shows that PI can be viewed as a method for model explanation which in between the scientific inference and feature selection approaches. The scientific inference approaches (MCI and UMFI) allocate all of the redundant information to the feature. The feature selection approaches (CPI and ablation) allocate none of the redundant information to the feature. PI evenly splits the redundant information across the relevant correlated features.

When tested with extremely randomized trees, the correlation simulation experiment results (Figure 8g) for MCI and UMFI change slightly compared to the experiment with random forests in Figure 1c. MCI works well, though it still gives some non-zero importance to x_4. With random forests, the relative importance of x_4 was usually above 5%, but with extremely randomized trees, the relative importance dropped below 5%. The performance of UMFI with linear regression got slightly worse as now the importance of x_1 is slightly greater than that of x_2 on average. The performance of UMFI with optimal transport changed for the better and now the importance of x_1 and x_2 are almost identical which was not true before. In

this experiment, UMFI_OT performed the best.

G.1.4 Blood relation

For the last simulation experiment, we revisit the blood relation experiment performed in Section 4.1.4 using data generated from the causal graph in Figure 2. The feature S is unobserved, so the only blood related features to Y in F are x_3 and x_4. x_3 and x_4 should therefore be given high importance while x_1 and x_2 should receive zero importance. When tested on ablation, CPI, and PI, we notice that all three metrics fail to capture the desired importance, since they each give significant importance to x_2, which is not blood related to Y. We also note that this experiment provides an explicit example of UMFI not satisfying the marginal contribution axiom, which states that feature importance metrics should allocate at least as much importance as attributed by the ablation metric. Indeed, as shown in Figure 1d, UMFI gives around zero importance to non-blood related features x_1 and x_2, whereas ablation gives a significant portion of the importance to x_2.

When MCI and both implementations of UMFI were re-tested using extremely randomized trees instead of random forest, we observe that UMFI_LR and UMFI_OT both continue to give positive importance to the blood related features x_3 and x_4, while giving near-zero importance to the two remaining observed features (Figure 8h). However, we note that x_3 is given much more importance relative to x_4 when implemented with extremely randomized trees compared to random forests (Figure 1d). On the other hand, MCI gives positive importance to x_2 in this experiment. We note that MCI correctly gave x_1 almost zero importance while giving x_3 and x_4 significantly more importance compared to the random forest implementation. Across most simulation studies, it appears MCI performs slightly better using extremely randomized trees compared to random forests.

G.2 Extra BRCA experiments with known ground-truth feature importance

The following experiments are performed on the BRCA dataset with 571 patients, each with one of four breast cancer subtypes, and 50 continuous predictor genes. The experiments use the same setting as in Section 4.2, where the 40 randomly chosen genes are also permuted so that the ground-truth feature importances are known. We observed that the overall classification accuracy of random forests for this dataset was 0.76.

G.2.1 Running 5000 iterations of UMFI

The original BRCA experiment conducted in Section 4.2 showed that UMFI_LR and UMFI_OT performed impressively on real data, providing significantly more accurate feature importance scores than MCI after 200 iterations of the experiment. Both UMFI_LR and UMFI_OT correctly gave high importance to the ten BRCA-associated genes, while giving zero median importance to about 80% of the unassociated genes. Additionally, in an overnight study spanning less than ten hours, UMFI_LR and UMFI_OT displayed ideal results after running 5000 iterations of the BRCA experiment. As shown in Figure 9, both implementations of UMFI achieve 100% overall accuracy by giving high importance to the ten BRCA-associated genes and zero median feature importance to all 40 unassociated genes. These results indicate that UMFI's relatively low computational cost can be leveraged via aggregation to achieve superior performance on complex data within a reasonable time budget.

G.2.2 Ablation, PI, and CPI

We also test the quality and robustness of other feature importance metrics including ablation, PI, and CPI, by running 200 iterations of the BRCA experiment from Section 4.2 for each method. Results are shown in Figure 10. Ablation importance scores are small and have large uncertainties compared to its median importance scores, which makes the scores impractical to interpret. Eight of the ten important genes are identified by ablation, but all other genes are given exactly zero median importance. All ten important genes are given non-zero importance by CPI, however, some randomly permuted genes are given more importance than some genes known to be important, such as CDK6. PI gave more reliable and stable results compared to ablation and CPI in this experiment, exhibiting similar performance to UMFI_LR and UMFI_OT from the analogous experiment shown in Figure 3. We note that PI assigned zero importance to 29 of the 40 unassociated genes, making its TNR of 0.725 slightly lower than UMFI in the analogous experiment from Section 4.2.

G.3 Experiments on unpermuted BRCA data

Additional BRCA experiments were performed on the original unpermuted genes, as done in Covert et al. (2020) and Catav et al. (2021). The observed overall classification accuracy of random forests for this dataset was 0.79.

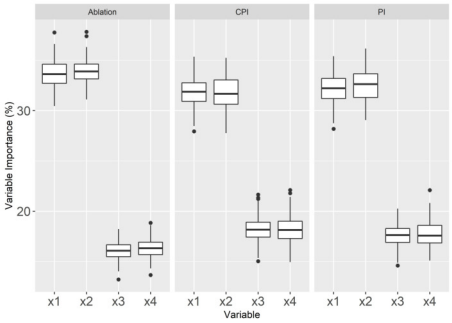

(a) RF: Nonlinear interactions

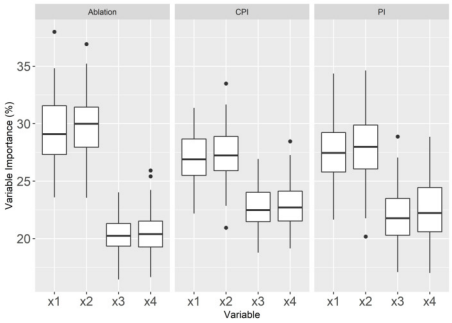

(b) RF: Correlated interactions

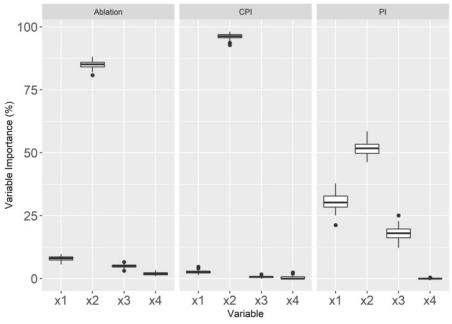

(c) RF: Correlation

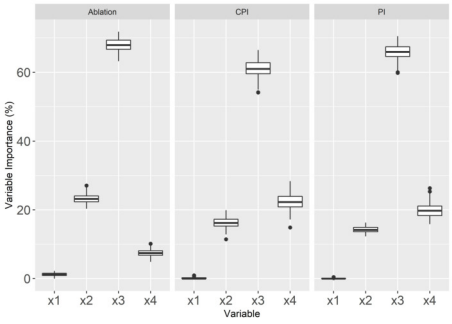

(d) RF: Blood relation

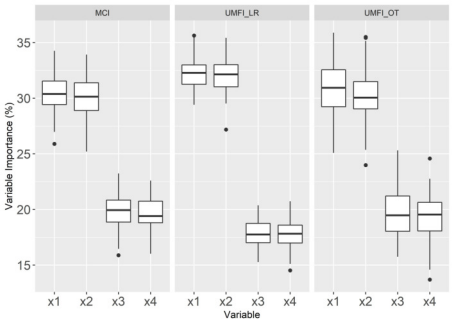

(e) ET: Nonlinear interactions

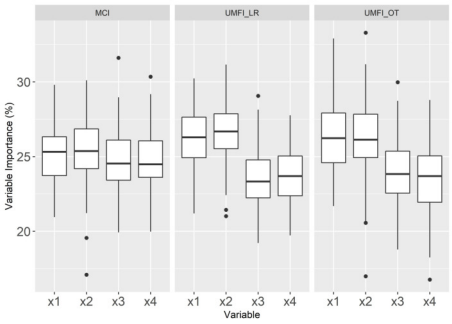

(f) ET: Correlated interactions

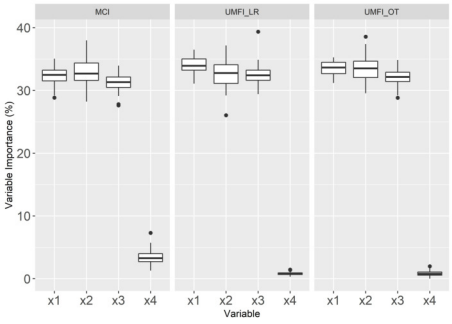

(g) ET: Correlation

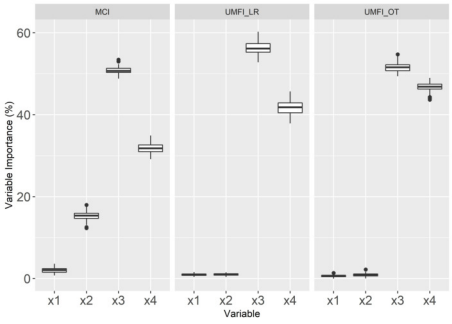

(h) ET: Blood relation

Figure 8: Results for the experiments on simulated data from Subsection G.1. The results for ablation, conditional permutation importance (CPI), and permutation importance (PI) were implemented with random forest (RF), and are shown in Figures 8a, 8b, 8c, and 8d . The results for MCI, UMFI_LR, and UMFI_OT were implemented with extremely randomized trees (ET), and are shown in Figures 8e, 8f, 8g, and 8h. Feature importance scores are shown as a percentage of the total for each of x_1 to x_4 from 100 replications.

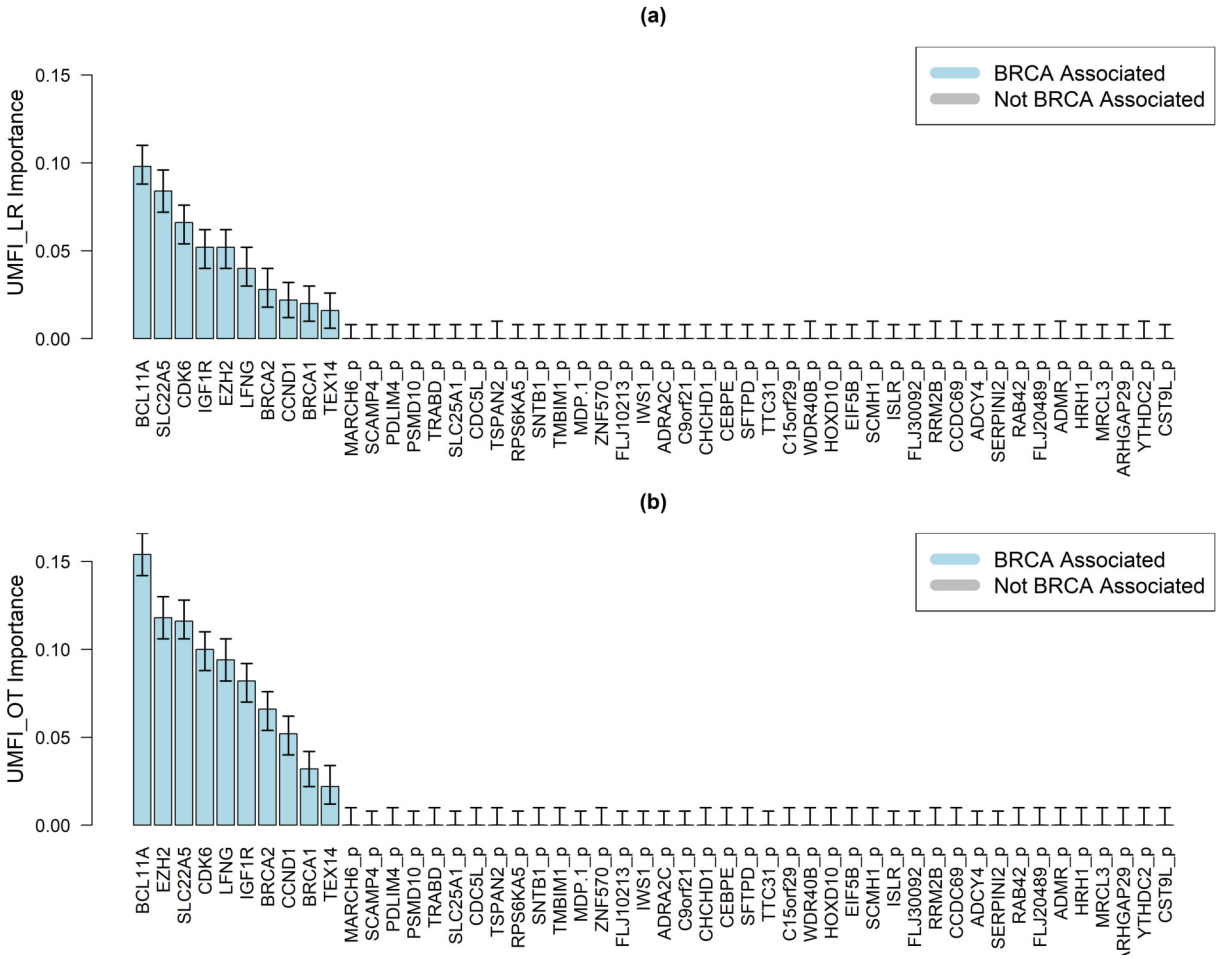

Figure 9: Median feature importance scores provided by (a) UMFI with linear regression, and (b) UMFI with pairwise optimal transport, for each gene in the permuted BRCA dataset after 5000 iterations. Genes colored in blue are known to be associated with breast cancer while genes colored in grey are random permutations of randomly selected genes, which we assume to be unassociated with breast cancer subtype. The first and third quantiles of the scores are visualized for each gene.

Feature importance scores on this dataset were first computed with MCI, UMFI_LR, and UMFI_OT over 100 iterations, as shown in Figure 11. The ordering of the BRCA associated genes is fairly similar across MCI and both UMFI methods. BCL11A and SLC22A5 are always the top two features and TEX14 is always the least important BRCA associated gene. While there are clear similarities in the results of all methods, the glaring difference is the number of features given zero importance. While MCI gives non-zero median importance to all 50 features, 14 features are given zero median importance by UMFI with linear regression, and 10 features are given zero median importance by UMFI with pairwise optimal transport. It is unlikely that all 40 randomly selected genes, which have not shown any association with breast cancer in previous studies, share information about breast cancer, so in this respect, we conclude that UMFI performs better than MCI.

Feature importance scores on the unpermuted BRCA dataset were also computed with ablation, CPI, and PI over 100 iterations, as shown in Figure 12. When also considering these results, we observe that MCI, UMFI, and PI give similar importance scores, while ablation and CPI performed significantly worse. Once again, ablation's high relative variance hampers its interpretability. Meanwhile, CPI gave by far the highest importance to SLC25A1, which is not known to have any association with breast cancer. In the results of MCI, UMFI, and PI, BCL11A is the most important while CST9L is always among the most important non-BRCA associated genes. Contrary to this, ablation and CPI give high importance to BRCA1, BRCA2, TEX14, EZH2, and IGF1R for BRCA associated genes, and SLC25A1 for non-BRCA associated genes.

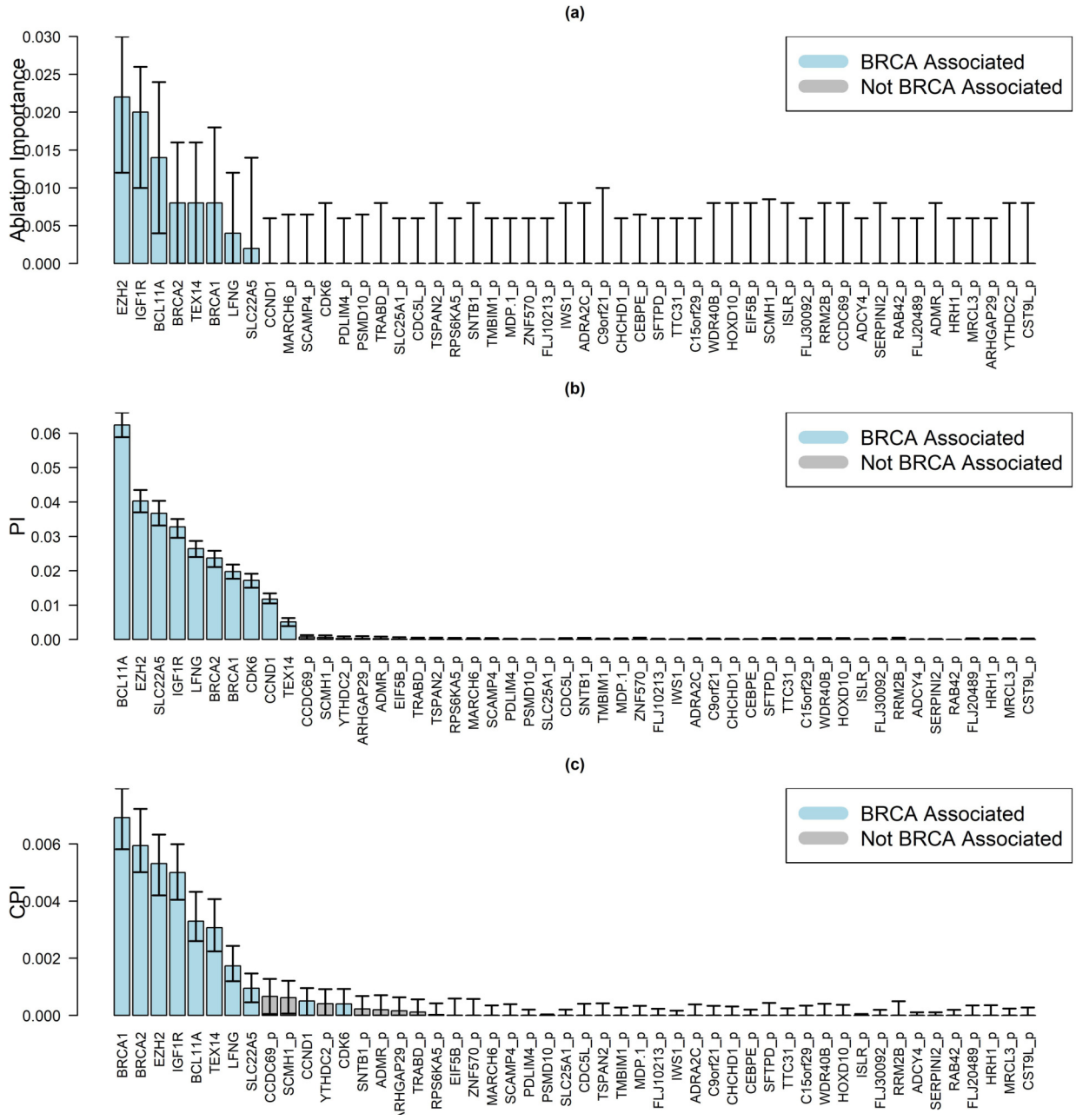

Figure 10: Median feature importance scores provided by (a) ablation, (b) permutation importance, and (c) conditional permutation importance, for each gene in the permuted BRCA dataset after 200 iterations. Genes colored in blue are known to be associated with breast cancer while genes colored in grey are random permutations of randomly selected genes, which we assume to be unassociated with breast cancer subtype. The first and third quantiles of the scores are visualized for each gene.

G.3.1 Computational complexity

We compare the computational complexity of UMFI and MCI against the other feature importance methods that were explored in this section: ablation, PI, and CPI. To do so, we ran 10 iterations of the BRCA experiment, which has 50 features, each with 571 observations. We recorded the average time for each method to compute feature importance for $5, 10, 15, 20, 25, 30, 35, 40, 45$, and 50 features. Figure 13 shows that PI is the fastest method, processing 50 features in 50 milliseconds on average, followed by ablation (50 features in 1.8 seconds), UMFI (50 features in 3 seconds when

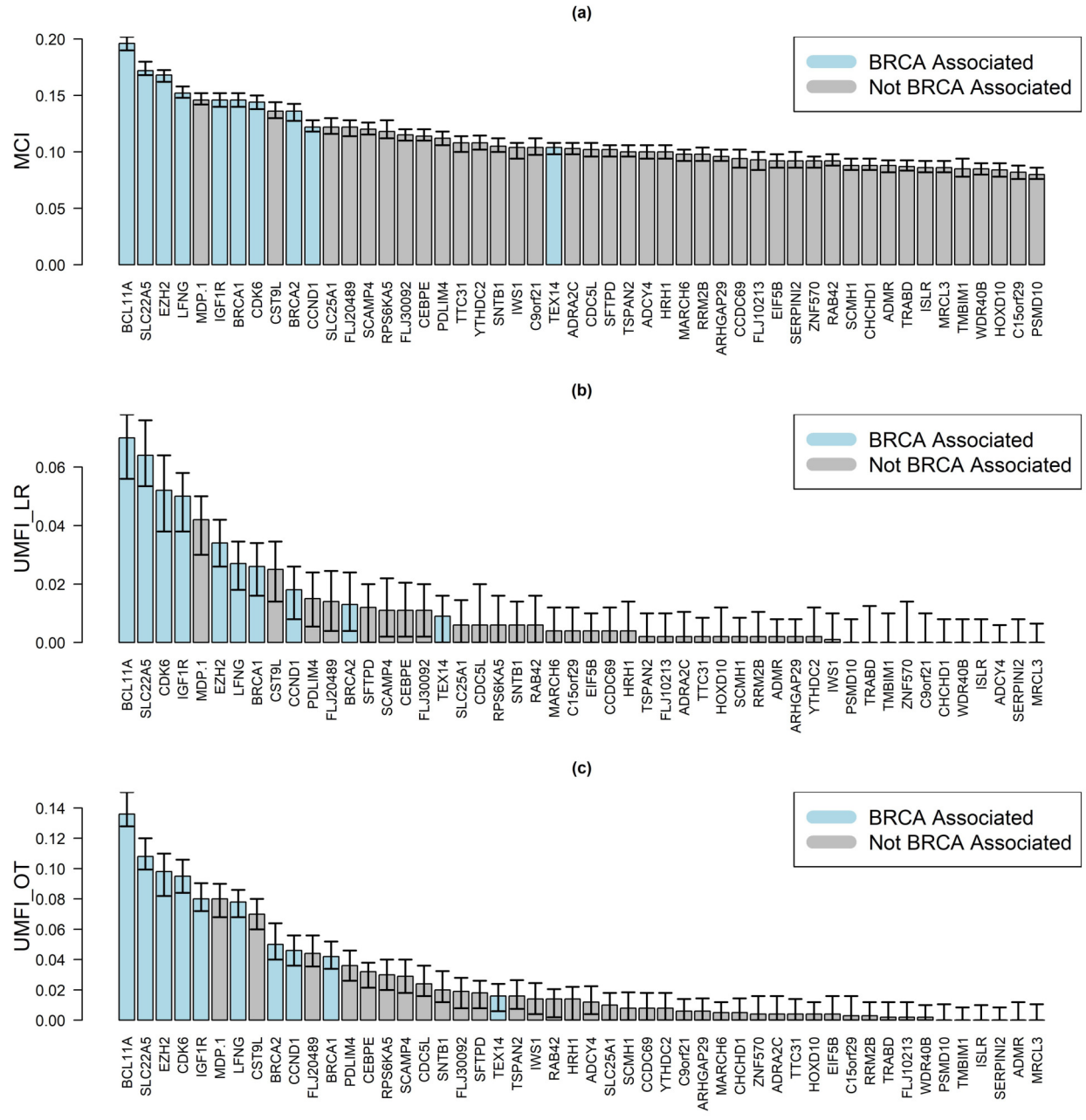

Figure 11: Median feature importance scores provided by (a) MCI, (b) UMFI with linear regression, and (c) UMFI with pairwise optimal transport, for each gene in the unpermuted BRCA dataset after 100 iterations. Genes colored in blue are associated with breast cancer while genes colored in grey are randomly selected genes. The first and third quantiles of the scores are visualized for each gene.

parallelized), CPI (50 features in 30 seconds), and finally MCI with soft 2-size submodularity (50 features in 205 seconds).

G.4 Experiments on hydrology data

The final experiments for this study were conducted on a large-sample hydrology dataset called CAMELS (Addor et al., 2017). This dataset records catchment averaged climate, soil, geology, topography, and land cover characteristics for 643 catchments across the contiguous United States. With these, there are 29 continuous explanatory variables. The response

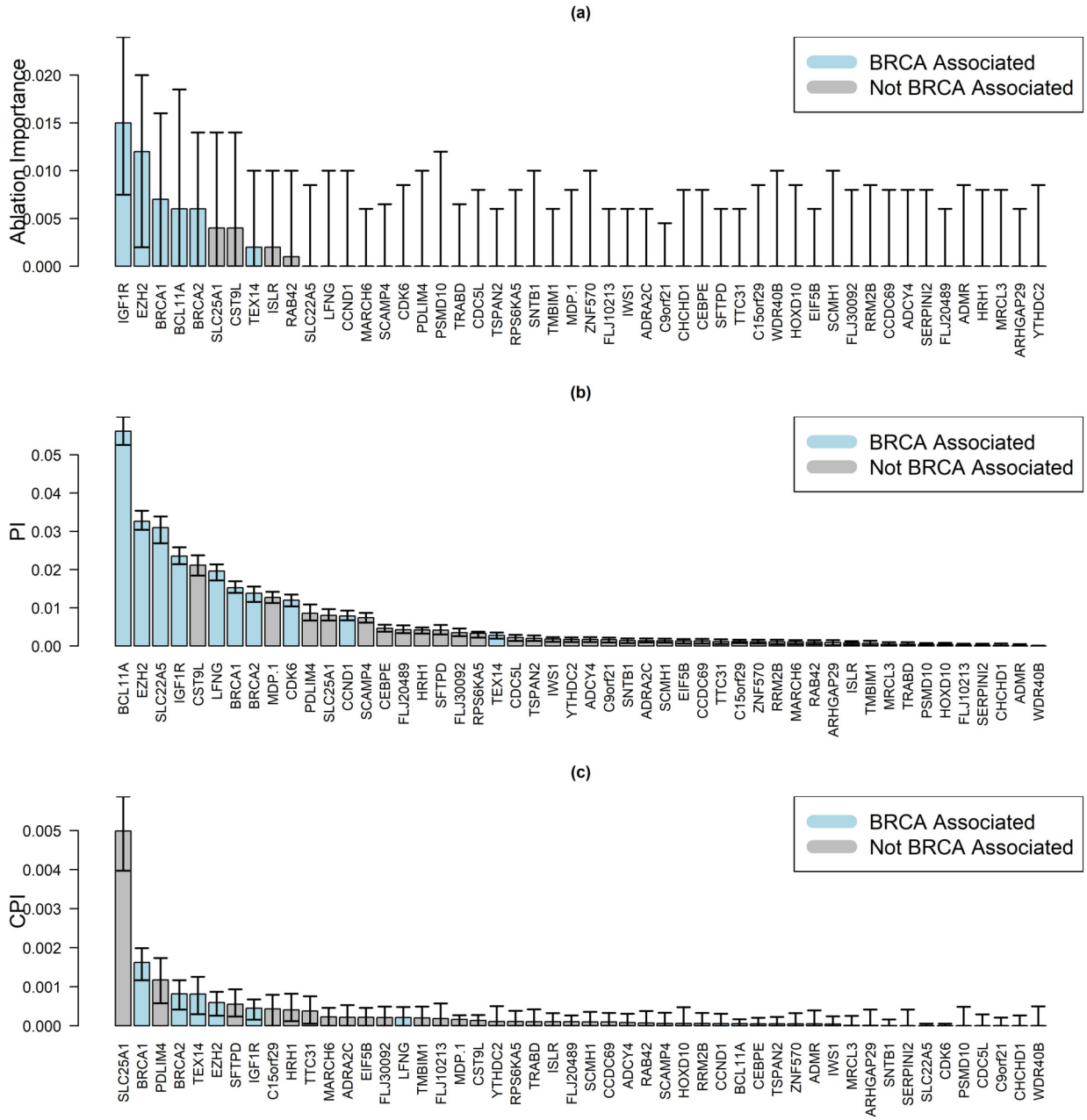

Figure 12: Median feature importance scores provided by (a) ablation, (b) permutation importance, and (c) conditional permutation importance, for each gene in the unpermuted BRCA dataset after 100 iterations. Genes colored in blue are associated with breast cancer while genes colored in grey are randomly selected genes. The first and third quantiles of the scores are visualized for each gene.

variable is averaged yearly streamflow, which is also continuous. Extremely randomized trees were used in this experiment with an overall OOB-R^2 of 0.91.

Figure 14, which is analogous to Figure 6 in Appendix F, shows that both preprocessing methods fail to completely remove dependencies from the CAMELS dataset. This can likely be attributed to the fact that each feature is extremely dependent on the other explanatory features ($R^2 \geq 0.65$).

The feature importance scores indicated in Figure 15 show that mean precipitation and aridity index are the features with

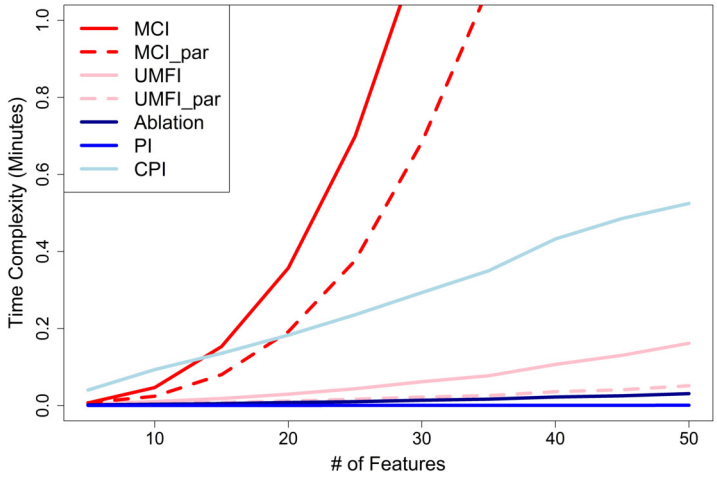

Figure 13: The average computation time for each method to process p features over 10 iterations of the original BRCA data is plotted for each $p \in \{5, 10, 15, 20, 25, 30, 35, 40, 45, 50\}$. We assume soft 2-size submodularity to run the MCI results.

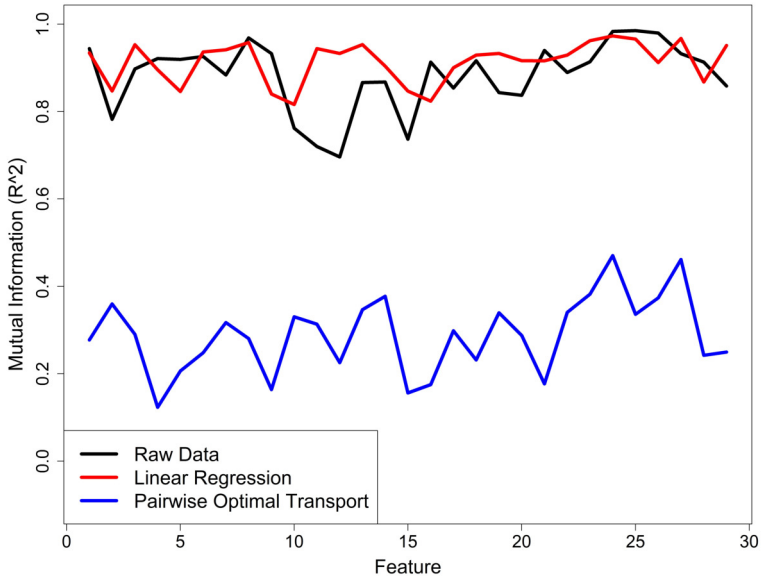

Figure 14: The coefficient of determination (random forest OOB-R^2) between the ith feature in the CAMELS dataset and all other features is plotted (black) for each $i \in \{1, 2, ...30\}$. The R^2 value between the ith feature and all other features after preprocessing with linear regression (red) and optimal transport (blue) is also plotted.

the strongest relationships with mean annual streamflow. Geology and soil attributes such as bedrock permeability and soil porosity are always among the least important features. These conclusions are in line with previous studies (Addor et al., 2018; Jehn et al., 2020), thus, even when dependencies can not be completely removed, UMFI can still provide reasonable measurements of feature importance.

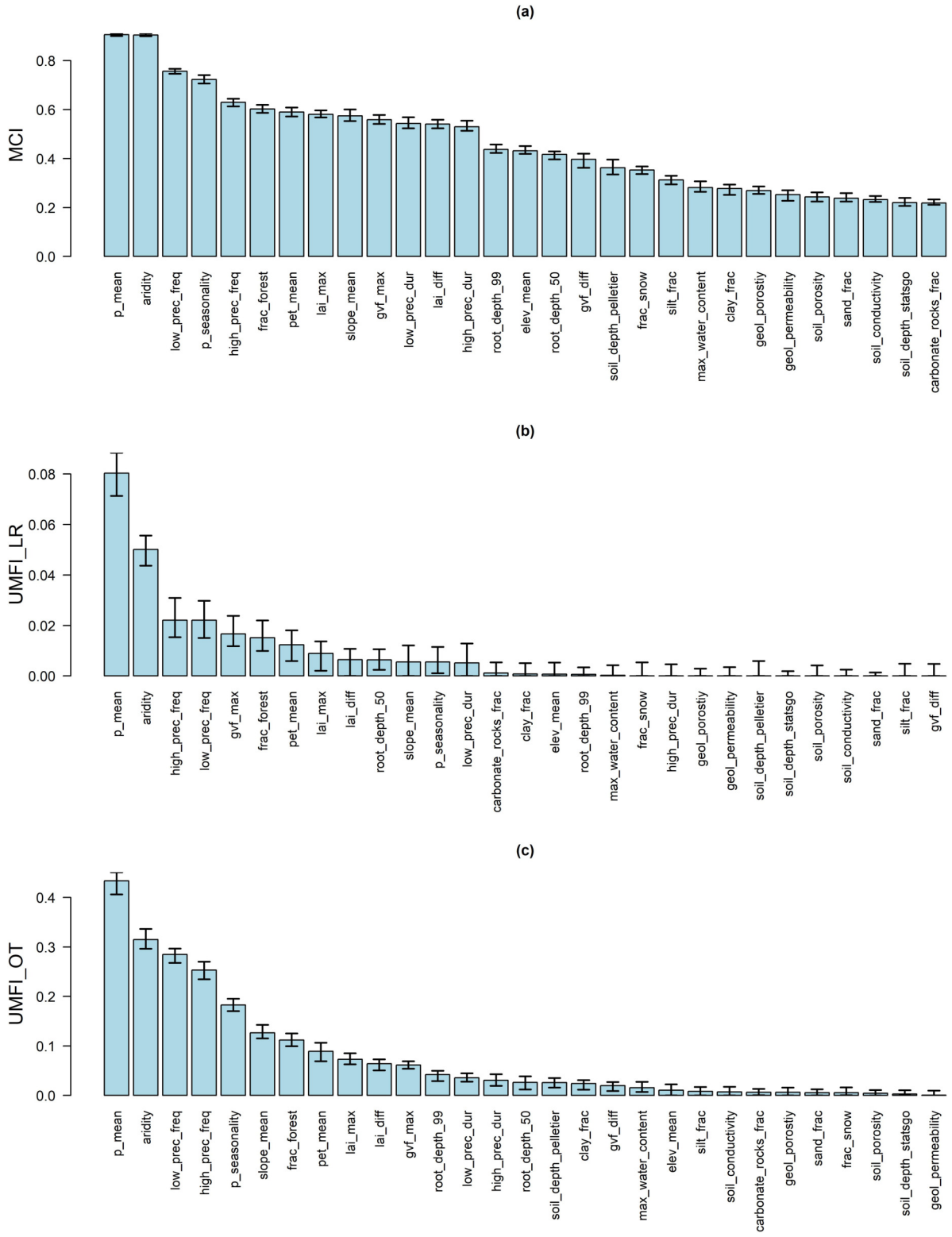

Figure 15: Median feature importance scores provided by (a) MCI, (b) UMFI with linear regression, and (c) UMFI with pairwise optimal transport, for each explanatory variable in the CAMELS dataset, aggregated after 100 iterations. The first and third quantiles of the scores are visualized for each feature.